NAVAL POSTGRADUATE SCHOOL

MONTEREY, CALIFORNIA

THESIS

IMAGING AND REFLECTANCE SPECTROSCOPY FOR THE EVALUATION OF EFFECTIVE CAMOUFLAGE IN THE SWIR

by

Ho Chee Leong

December 2007

Thesis Advisor:	Nancy Haegel
Co-Advisor:	Gamani Karunasiri

Approved for public release; distribution is unlimited

THIS PAGE INTENTIONALLY LEFT BLANK

REPORT DOCUMENTATION PAGE		Form Approved OMB No. 0704-0188

1. AGENCY USE ONLY *(Leave blank)*	2. REPORT DATE December 2007	3. REPORT TYPE AND DATES COVERED Master's Thesis

4. TITLE AND SUBTITLE Imaging and Reflectance Spectroscopy for the Evaluation of Effective Camouflage in the SWIR	5. FUNDING NUMBERS
6. AUTHOR(S) Ho Chee Leong	
7. PERFORMING ORGANIZATION NAME(S) AND ADDRESS(ES) Naval Postgraduate School Monterey, CA 93943-5000	8. PERFORMING ORGANIZATION REPORT NUMBER
9. SPONSORING /MONITORING AGENCY NAME(S) AND ADDRESS(ES) N/A	10. SPONSORING/MONITORING AGENCY REPORT NUMBER

11. SUPPLEMENTARY NOTES The views expressed in this thesis are those of the author and do not reflect the official policy or position of the Department of Defense or the U.S. Government.

12a. DISTRIBUTION / AVAILABILITY STATEMENT Approved for public release; distribution unlimited	12b. DISTRIBUTION CODE

13. ABSTRACT (maximum 200 words)

The emergence of SWIR (short-wave infrared) sensors and ongoing development of multi-spectral imagers that operate across four wavebands (visible, NIR, SWIR and MWIR) pose new challenges for current camouflage, concealment and deception technologies. For one, they render ineffective conventional camouflage material that worked well in the visible part of the spectrum. The aim of this thesis is to propose means to provide effective camouflage across the visible and SWIR spectrum. A system was developed for combined imagery and spectral reflectance measurements for the visible and the SWIR regions. The system utilizes an InGaAs focal plane array with a response range from 400 to 1700 nm. Experiments were conducted to study the reflectance of materials (e.g. foliage and current camouflage materials) across the two spectrums. From these experiments, the desired properties for camouflage materials were established. It is then proposed that a layer of nanomesh be used to complement current camouflage material in order to maintain the reflectance contrast between various dyes in the SWIR. The modified camouflage material would be reinforced with fibers tuned to absorb radiation around 1.4 μm wavelength. This would mimic the SWIR reflectance behavior exhibited by water contained in foliage. The proposed material will enhance the survivability of future warriors by providing effective camouflage across the visible and SWIR spectrums.

14. SUBJECT TERMS Shortwave Infrared, SWIR, SWIR imaging, SWIR Reflectance, Camouflage, Multi-spectral imaging, Wavelength tunable fibers, Chameleon fibers	15. NUMBER OF PAGES 85
	16. PRICE CODE

17. SECURITY CLASSIFICATION OF REPORT	18. SECURITY CLASSIFICATION OF THIS PAGE	19. SECURITY CLASSIFICATION OF ABSTRACT	20. LIMITATION OF ABSTRACT
Unclassified	Unclassified	Unclassified	UU

Standard Form 298 (Rev. 8-98)
Prescribed by ANSI Std. Z39.18

THIS PAGE INTENTIONALLY LEFT BLANK

Approved for public release; distribution is unlimited

IMAGING AND REFLECTANCE SPECTROSCOPY FOR THE EVALUATION OF EFFECTIVE CAMOUFLAGE IN THE SWIR

Ho Chee Leong
Major, Singapore Armed Forces (Army)
B.Eng., National University of Singapore, 2001

Submitted in partial fulfillment of the
requirements for the degree of

**MASTER OF SCIENCE IN
COMBAT SYSTEMS SCIENCES AND TECHNOLOGY**

from the

**NAVAL POSTGRADUATE SCHOOL
December 2007**

Author: Ho Chee Leong

Approved by: Nancy Haegel
Thesis Advisor

Gamani Karunasiri
Co-Advisor

James Luscombe
Chairman, Department of Physics

THIS PAGE INTENTIONALLY LEFT BLANK

ABSTRACT

The emergence of SWIR (short-wave infrared) sensors and ongoing development of multi-spectral imagers that operate across four wavebands (visible, NIR, SWIR and MWIR) pose new challenges for current camouflage, concealment and deception technologies. For one, they render ineffective conventional camouflage material that worked well in the visible part of the spectrum. The aim of this thesis is to propose means to provide effective camouflage across the visible and SWIR spectrums. A system was developed for combined imagery and spectral reflectance measurements for the visible and the SWIR regions. The system utilizes an InGaAs focal plane array with a response range from 400 to 1700 nm. Experiments were conducted to study the reflectance of materials (e.g. foliage and current camouflage materials) across the two spectrums. From these experiments, the desired properties for camouflage materials were established. It is then proposed that a layer of nanomesh be used to complement current camouflage material in order to maintain the reflectance contrast between various dyes in the SWIR. The modified camouflage material would be reinforced with fibers tuned to absorb radiation around 1.4 μm wavelength. This would mimic the SWIR reflectance behavior exhibited by water contained in foliage. The proposed material will enhance the survivability of future warriors by providing effective camouflage across the visible and SWIR spectrums.

THIS PAGE INTENTIONALLY LEFT BLANK

TABLE OF CONTENTS

LIST OF FIGURES

LIST OF TABLES

THIS PAGE INTENTIONALLY LEFT BLANK

ACKNOWLEDGMENTS

The author would like to express his appreciation to Mr Austin Richards from FLIR Systems (Commercial Vision Systems) for providing the motivation for this thesis research.

Also many thanks to Yoel Fink et al., School of Materials Science & Engineering at Massachusetts Institute of Technology (MIT) and Richard V. Gregory et al., School of Materials Science and Engineering, Clemson University, for allowing the author to carry out experiments on the fibers the respective groups have produced.

The author is also grateful for the support from everyone working in Professor Nancy Haegel's laboratory for their assistance and support. MAJ Alex Ang must be specially mentioned for the great advices he gave in MATLAB programming. The author would like to thank Professor Gamani Karunasiri for his guidance, advice and for being a mentor throughout his stay in Naval Postgraduate School. Most importantly, utmost gratitude to Professor Nancy Haegel for her guidance, support and the many insights in experimental work. It has truly been an enlightening experience working with an outstanding physics professor.

Last but not least, the author would like to thank his wife, Anna, and their two beautiful children, Bennett and Jonathan, for their love and support.

This work was supported in part by a contract from the Rapid Reaction Technology Office of the Office of the Secretary of Defense, DDR&E.

THIS PAGE INTENTIONALLY LEFT BLANK

I. INTRODUCTION

A. INEFFECTIVE CAMOUFLAGE IN SWIR

Infrared (IR) sensors traditionally operate in the mid-wave infrared (MWIR) and the long-wave infrared (LWIR) regions. There are two main reasons for widespread application of sensors in these two wavebands. The first motivation is the strong emission from human targets in the LWIR and the huge signature from targets like tanks and aircraft in the MWIR. The second reason is that radiation in the two wavebands is not severely affected by atmospheric attenuation.

In recent years however, sensors operating in the short-wave infrared (SWIR) region have emerged. The main motivation of having a sensor operating in this part of the spectrum is that it allows our soldiers to see eye-safe targeting lasers which have a typical wavelength of 1.55 μm. Also, having SWIR sensors provides an option for covert signaling beyond the range of increasingly proliferated Night Vision Devices (NVD) technology. Convert signaling or targeting devices operating in parts of the near-IR (NIR band is from 0.7-1.1 μm) region can now be seen by anyone with current or older generations of NVD. The advantage of being able to operate at night can be regained if there exists covert signaling means in the SWIR.

With technology available to sense in the SWIR, multi-spectral sensors operating across four wavebands (visible, NIR, SWIR and MWIR) are being developed. One reason for having these multi-spectral sensors is their ability to defeat conventional camouflage material. The contrast in reflectivity between the various dyes used for visible patterning diminishes in the SWIR. This causes the camouflage pattern to “disappear”. Furthermore, the camouflage material’s reflectance of SWIR does not match that of an environment with foliage in the

background. As a result, a target in camouflage material appears starkly bright, in contrast with the otherwise dark background created by the strong absorption of water contained in foliage.

B. PURPOSE OF THESIS

Current technologies in Camouflage, Concealment, and Deception (CC&D) that used to work in the visible spectrum are rendered ineffective with the emergence of SWIR and multi-spectral sensors. The aim of this thesis is to propose means to provide effective camouflage in both the visible and SWIR spectrums. The first step towards achieving the aim would be to develop a system for combined imagery and spectral reflectance measurements for the visible and the SWIR regions. Experiments can then be conducted to learn about materials' reflectance in the two wavebands. The system will allow the relevant spectral measurements to verify the effectiveness of proposed methods in providing camouflage across the visible and SWIR spectrums.

C. MILITARY RELEVANCE

The Defense Advanced Research Projects Agency (DARPA) has an ongoing program named the Multi-spectral Adaptive Networked Tactical Imaging System (MANTIS). The program aims to develop a helmet-mounted camera that captures images in the four wavebands (visible, NIR, SWIR and MWIR) and provides soldiers with a fused image on their helmets' visors [1]. Advanced NVG (ANVG) is another program that aims to extend the spectral response of current NVD into the SWIR. The successful fielding of such sensors will no doubt increase target detection and recognition rates. Potential adversaries may eventually have similar programs that allow their soldiers to have enhanced images combined from various spectral regions. Hence early research and development of camouflage material that works in the SWIR is critical to enhance the protection of our soldiers.

D. THESIS OVERVIEW

Chapter I provides an introduction to the thesis, outlining the purpose of the thesis, as well the military relevance of the work. Chapter II provides the background to the thesis by summarizing the impetus for development of SWIR sensors. It highlights the material and technology that enable sensing in the SWIR and define the need for effective camouflage in the SWIR. Chapter III describes the system developed for combined imagery and spectral reflectance measurements for the visible and the SWIR regions. It details how reflectance measurements were taken and computed using various software. Chapter IV consists of a synopsis on conventional camouflage technique. The chapter also contains key experimental results that shows the reflectance of foliage in the SWIR. From that experiment, materials properties for effective camouflage in the visible and SWIR were established. Chapter V includes an explanation of how the effectiveness of camouflage can be enhanced by having a layer of wearable nanomesh, interlaced with conventional camouflage material. Chapter VI explores the idea of using wavelength tunable fibers to further mimic the environment. These fibers can be used to reinforce the new camouflage material by simulating water absorption around 1.4 μm. This will deteriorate the ability of multi-spectral imagers to defeat the new camouflage material. Finally, Chapter VII summarizes the thesis and offers suggestions for further research.

THIS PAGE INTENTIONALLY LEFT BLANK

II. SWIR TECHNOLOGY

A. SHORTWAVE INFRARED (SWIR) SENSING

For military applications, IR sensors refers to sensors whose response falls within the 0.7 to 14 micrometers (μm) region. Three sub-regions, with acceptable amount of atmospheric transmittance for IR sensing, are defined within the IR spectral range. Figure 1 shows the atmospheric transmission over a 1 km path length as a function of wavelength in the IR. The short-wave infrared (SWIR) region is from 0.7 to 2.5 μm, while the mid-wave infrared (MWIR) and long-wave infrared (LWIR) windows are 3-5 μm and 8-12 μm respectively.

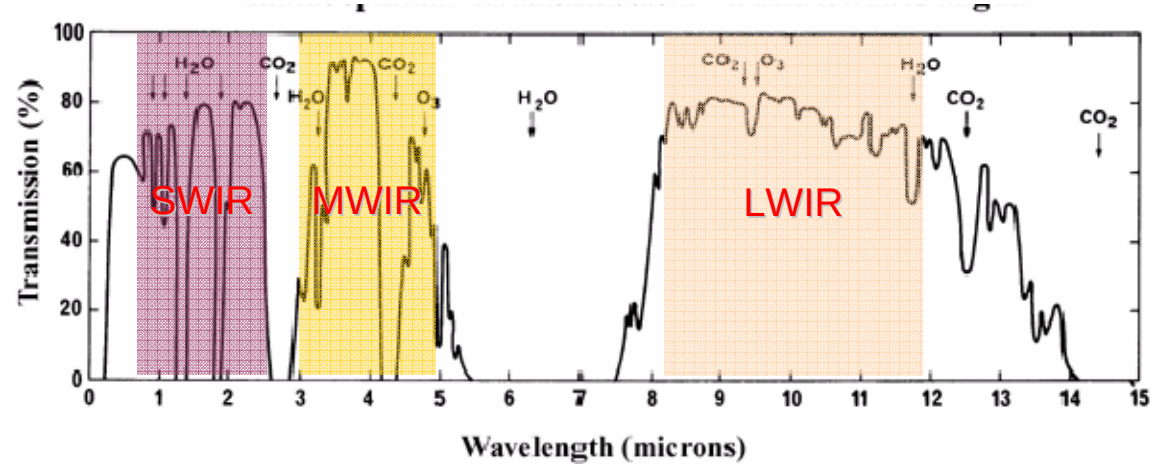

Figure 1. Atmospheric transmission – 1 km path length (From [2])

Traditionally, military IR sensors were developed to exploit the MWIR and LWIR wave bands. This is because military targets generally emit strongly in these two regions. Based on Wien's displacement law, a human target, typically modeled as a 310K blackbody, emits strongly in the LWIR with the peak emission around 10 μm. Tanks and aircraft engines have temperatures on the space order of 1000 K; therefore they emit strongly in the MWIR region, with peak emission around 3 μm. For MWIR and LWIR sensors, the emissivity of the

targets is a key parameter [3]. When the targets and the background are of the same temperature, the difference in emissivity enables IR sensors to differentiate targets from background.

More recently, compact semiconductor focal plane array military sensors have been developed in the SWIR. One reason is because the sun and stars have strong emission in this wave band. SWIR sensors, like the image intensifiers which operate in the visible and near-IR (NIR band is from 0.7-1.1 μm) region, can convert photons from reflected sunlight, moonlight or starlight off targets, into electrons and back to photons for display purpose. Hence, the important target parameter for SWIR sensors is the targets' reflectivity. Cameras in the visible, NIR and SWIR regions are broadly categorized as Electro-optics (EO) sensors and the reflectivity of the targets is exploited for sensing in these wave bands. The use of reflected light for sensing enables SWIR cameras to produce images close to that of human vision. Longer wavelength IR cameras, on the other hand, produce images that require interpretation by trained users.

There are two main motivations to have military sensors operating in the SWIR region. The first motivation is that it allows our soldiers to "see" eye-safe targeting laser operating at 1.55 μm. Lasers such as Nd:YAG (1.06 μm) are considered unsafe for the eye because the laser beam converges onto the retina and cause severe damage that may lead to blindness. Lasers at 1.55 μm are "eye-safe" because the beam does not converge onto the retina of the eye. In fact, light with wavelength longer than 1.4 μm is not transmitted through the cornea. These lasers at longer wavelength can however cause damage to the cornea but the damage may not be severe or permanent. Even if it is permanent, current medical technology is available for corneal transplant.

There is currently a technology gap because Night Vision Devices (NVD), which have a spectral response out to 0.9 μm, do not detect either the 1.06 or 1.55 μm targeting lasers. Indium Antimonide (InSb) detectors, traditionally used for sensing in 3-5 μm range, is used to "spot" such targeting lasers. Most laser-guided munitions are directed by Nd:YAG lasers and the sensitivity of InSb to

these lasers is quoted as less than 20% compared to its quantum efficiency at the 3-5 μm region [4]. More importantly, sensors made of InSb material require cooling, which increases both the weight and the cost of the sensor.

The second motivation of having sensors in the SWIR is to provide options for covert signaling beyond the range of increasingly proliferated NVD technology. With the proliferation of NVD technology, the U.S. military and its allies no longer completely owns the night. Convert signals or targeting lasers in part of the NIR region can now potentially be seen by adversaries. In the 2006 conflict between Israel and Lebanon, the terrorist group Hezbollah reportedly disrupted Israeli Special Forces conducting night operations because they too possessed NVD capability [5].

Another great advantage of having SWIR cameras is that they can be used from within vehicle windscreens because glass offers 90% transmittance from 0.3 to 2 μm. IR sensors currently employed have to be used outside the vehicle thus exposing observers to possible enemy fire. There is also great cost saving associated with the use of glass lenses for SWIR cameras. Glass lenses are cheaper and more readily available than the germanium (Ge) lenses required for MWIR and LWIR cameras.

Finally, SWIR sensors complement traditional IR cameras and enhance the probability of detecting targets hidden behind foliage. There is a strong absorption of IR radiation by water at 1.4 μm. IR radiation at this wavelength is absorbed because it matches the harmonic frequencies of OH-bond vibrations [6]. Foliage contains a high percentage of water. Hence, foliage materials can be distinguished from non-foliage materials by comparing an image taken in the visible spectral with one taken in the SWIR spectral [7].

Moreover, IR sensors in the MWIR and LWIR spectral have poor performance during thermal crossover times. Thermal crossover, defined as the time during the day when the thermal contrast is at a minimum and the polarity of the contrast reverses, generally occurs at midmorning and late afternoon. Based

on an experiment conducted U.S. Army Research Laboratory and Northrop Grumman, thermal crossover occurs at approximately 0900 and 1700 in winter, accounting for the low detection range of a tank target at those times [8]. This is an undesirable effect because the enemy may exploit this window of opportunity to conduct operations. Figure 2 illustrates the significant reduction in detection range during the thermal crossover times.

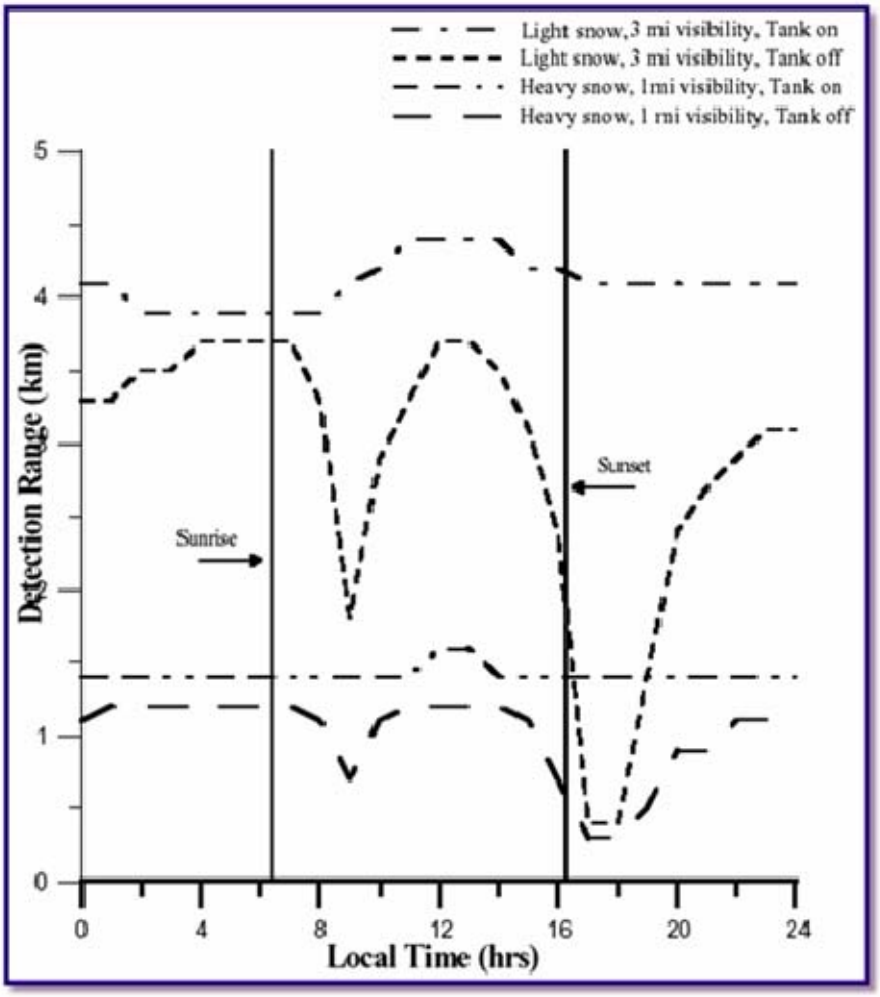

Figure 2. Detection Range of IR sensor at different times of the day (From [8])

SWIR sensors do not have similar behavior during thermal crossover period. This is because SWIR sensors do not depend on the thermal contrast between targets and background for detection. Instead, it depends on the targets' reflectivity, which do not change significantly during thermal crossover times. This, together with the other advantages mentioned above, makes SWIR sensors a good complement to traditional MWIR and LWIR sensors.

B. PHOTODETECTOR MATERIAL

Indium Gallium Arsenide (InGaAs) is the photodetector material used for detection in the SWIR. $In_xGa_{1-x}As$ is a ternary alloy which has a tunable cutoff wavelength between 0.87 and 3.75 µm, the cutoff wavelengths for its two parent alloys, GaAs and InAs respectively. The bandgap, cutoff wavelength and lattice constants of the ternary alloy changes by varying the composition of the two parent alloys.

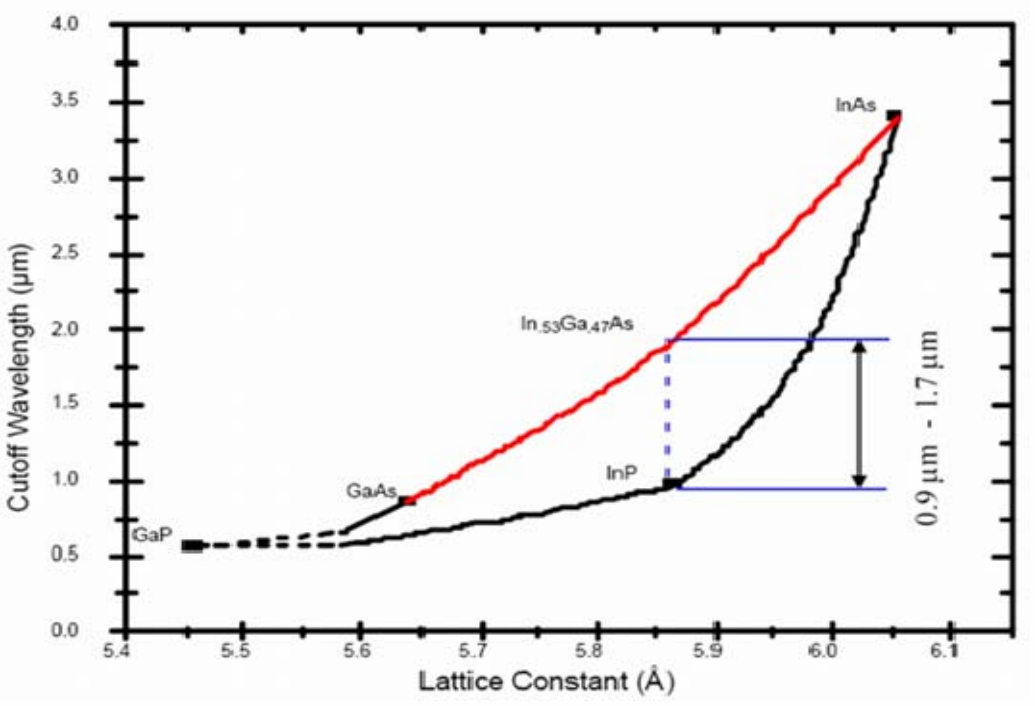

Figure 3. Plot of the cut-off wavelengths versus the lattice constant for InGaAs alloy (From [9])

$In_xGa_{1-x}As$ alloy is usually grown on a substrate with matching lattice constant to prevent the degradation of the material due to lattice-mismatch. In the production of InGaAs for SWIR detection, $In_{0.53}Ga_{0.47}As$ is lattice-matched and grown onto an Indium Phosphide (InP). $In_{0.53}Ga_{0.47}As$ photodiodes have cutoff wavelength of 1.7 µm while the InP substrate has a cut-off wavelength of 0.9 µm. Hence, the product is an InGaAs material, which has spectral response from 0.9 to 1.7 µm as shown in Figure 3.

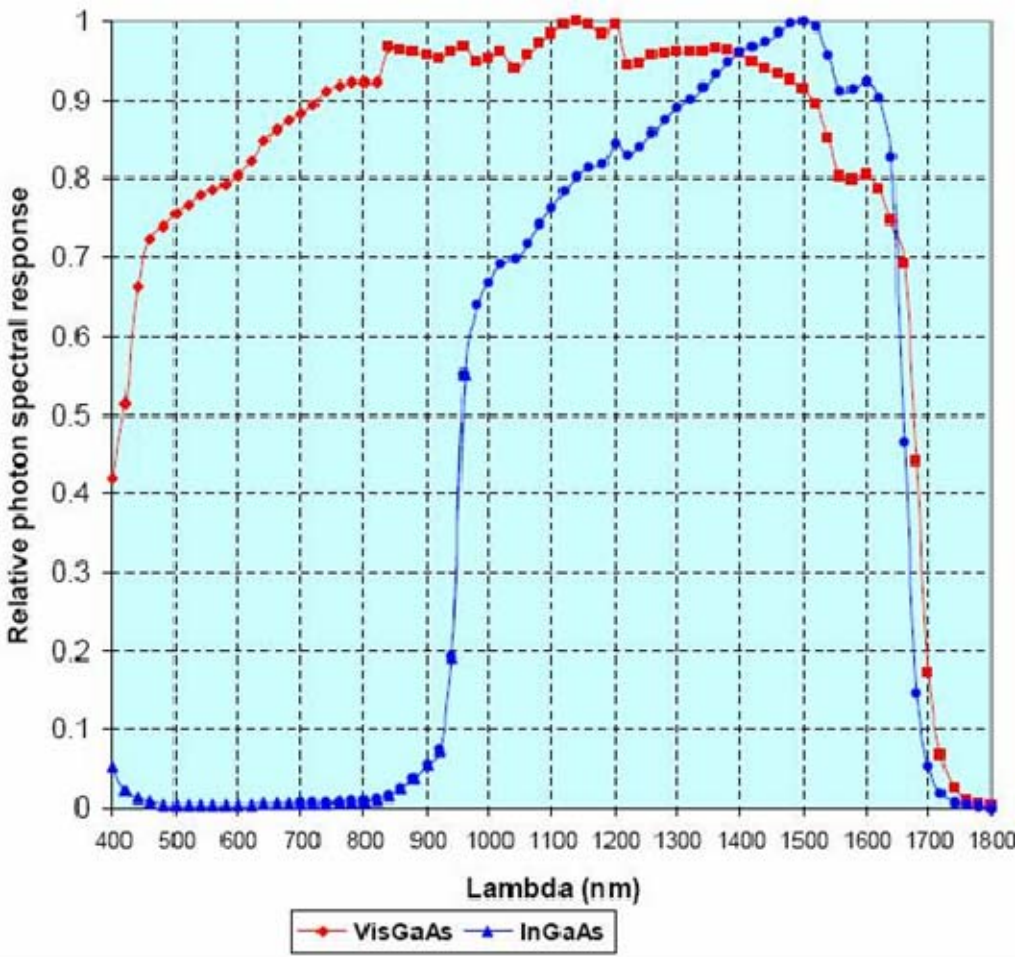

Figure 4. Spectral Response plotted against wavelength for InGaAs and VisGaAs materials produced by Indigo Systems Corporation (From [11])

Visible InGaAs or VisGaAs material has been developed by several companies for sensing in both the visible and the SWIR spectrum. The material is sensitive from 0.4 to 1.7 μm. VisGaAs is essentially InGaAs material with the InP substrate etched out to allow transmittance of visible light [10].

The etching process reduces the thickness of the InP substrate but does not remove it completely. The remaining thinned InP material allows visible light and NIR radiation to pass through, since the absorption coefficient is smaller for incident photons with less energy. However, absorption by the thinned InP increases with the energy of the incident photons. Also, the electron-hole pairs created by incident photons of higher energy tends to recombine near the surface before being collected. Therefore, the spectral response is insignificant for radiation lower than 0.4 μm. Figure 4 illustrates extended spectral response of the VisGaAs material produced Indigo Systems Corporation [11].

The performance of a photodetector material is limited by the noise or the temperature of the background. Detectivity, D*, is the figure of merit for the performance of photodetectors in a background limited environment. It is the measure of the sensitivity of the material, normalized to 1 cm^2 area and 1-Hz noise equivalent bandwidth.

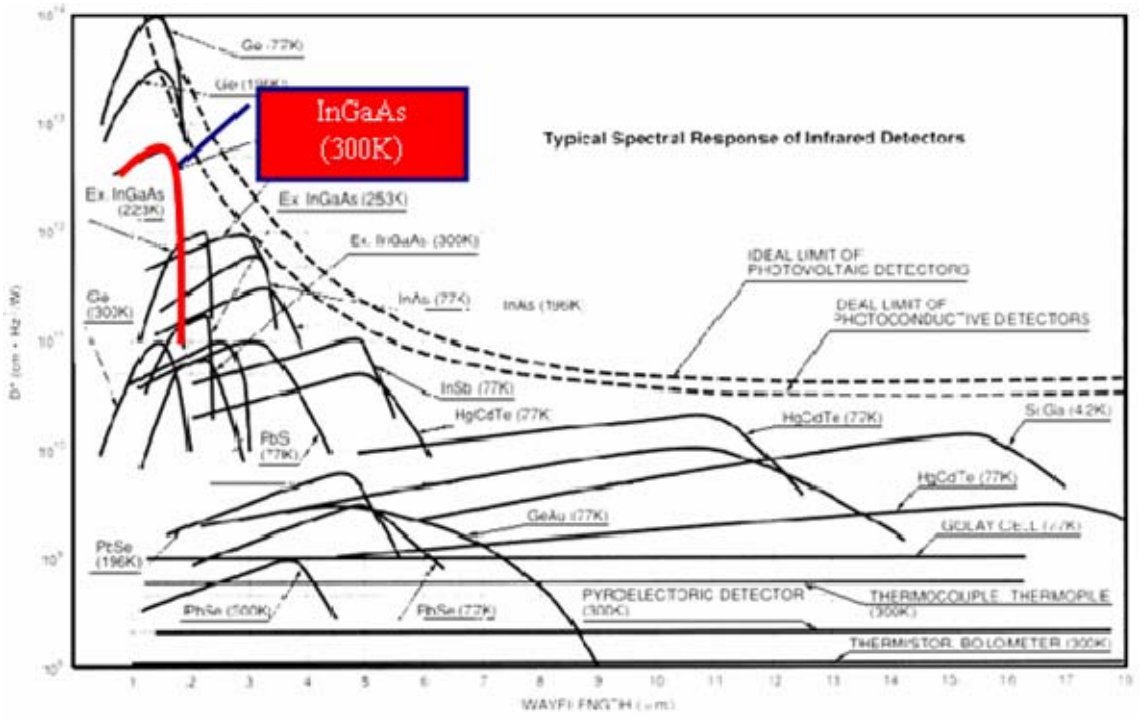

Figure 5. D* plotted against wavelength for Infrared Detectors (From [12])

The sensitivity of a detector can be increased by operating at lower temperature. However, cooling of military sensors increases the cost and more importantly, the weight of the sensor often carried by soldiers. As shown in Figure 5, InGaAs material has the advantage of possessing high D* at normal room temperature. High sensitivity at ambient temperature makes it an ideal material to produce SWIR cameras for military purposes.

C. DEVELOPMENT OF SWIR CAMERAS FOR THE MILITARY

The performance of EO and IR sensors is affected by environmental effects such as rain, fog or smoke. Each environmental effect degrades the performance of sensors in different wavebands to varying extent. No one sensor works best under all conditions. Sensor fusion is the way to mitigate the environmental effects of operating in a particular waveband. Multi-spectral sensor systems capture images in various wavebands. The images are processed using

software to produce a fused image. For example, the quality of an image captured in the visible and SWIR spectral may be severely degraded by presence of fog. The image will be significantly enhanced with information from the MWIR or LWIR spectral because sensors in these two wavebands are less affected by fog.

The Defense Advanced Research Projects Agency (DARPA) has a program named the Multi-spectral Adaptive Networked Tactical Imaging System (MANTIS). Based on the concept of sensor fusion mentioned above, the program aims to develop a helmet-mounted camera that capture images in the four bands, namely the visible, NIR, SWIR and LWIR, and provides soldiers with a fused image on their helmets' visors. So far, MANTIS was demonstrated in PC based hardware, performing the multi-sensor fusion in real-time using nine processors. The next phase currently in progress is developing the MANTIS Vision Processor (MVP), a much smaller 'system on a chip' that will be integrated into a helmet and hand held viewer [1]. This program, coupled with other programs to provide covert illumination and signaling means in the SWIR, greatly enhances the capability of soldiers to operate covertly in the night, regardless of the presence of battlefield obscurant or other environmental effects. Figure 6 shows a Liteye OLED Helmet Mounted Display developed as part of the MANTIS Program [13].

Figure 6. Liteye OLED Helmet Mounted Display developed as part of the MANTIS Program (From [13])

Multi-spectral sensor systems are also flown by manned and Unmanned Aerial Vehicles (UAVs). When used as a tool for covert surveillance, these sensor systems increase the chance for target detection, recognition and tracking. SWIR microcameras weighing only 17 grams have been produced by Goodrich Sensor Unlimited for this purpose [14]. These cameras, such as the one shown in Figure 7, measure only 5.9 X 2.8 X 1.7 cm^3 (about the size of a 9V battery) and fit right into an UAV.

Figure 7. SWIR camera produced by Sensor Unlimited flown on UAV (From [14])

There are other military programs involving the use of SWIR technology. Advanced NVG systems, for example, aim to extend the spectral response of NVDs from the NIR waveband into the SWIR [15]. Figure 8 illustrates the radiance of the night sky under different conditions. Radiance is noticeably lower in moonless nights because of the absence of reflected light from the sun. The radiance increases significantly with the visibility of the moon. There is a significant decrease in radiance around 1.4 μm. This is due to the absorption of the radiation at this wavelength by water content in the atmosphere. The high radiance in the SWIR region can be attributed to night glow, the irradiance emitted by the upper atomsphere. Night vision in low or no light conditions can therefore be greatly enhanced with extended spectral response in the SWIR. The development of compact InGaAs focal plane arrays is the key enabler to the assembly of helmet mounted image intensifiers that have extended spectral response in the SWIR.

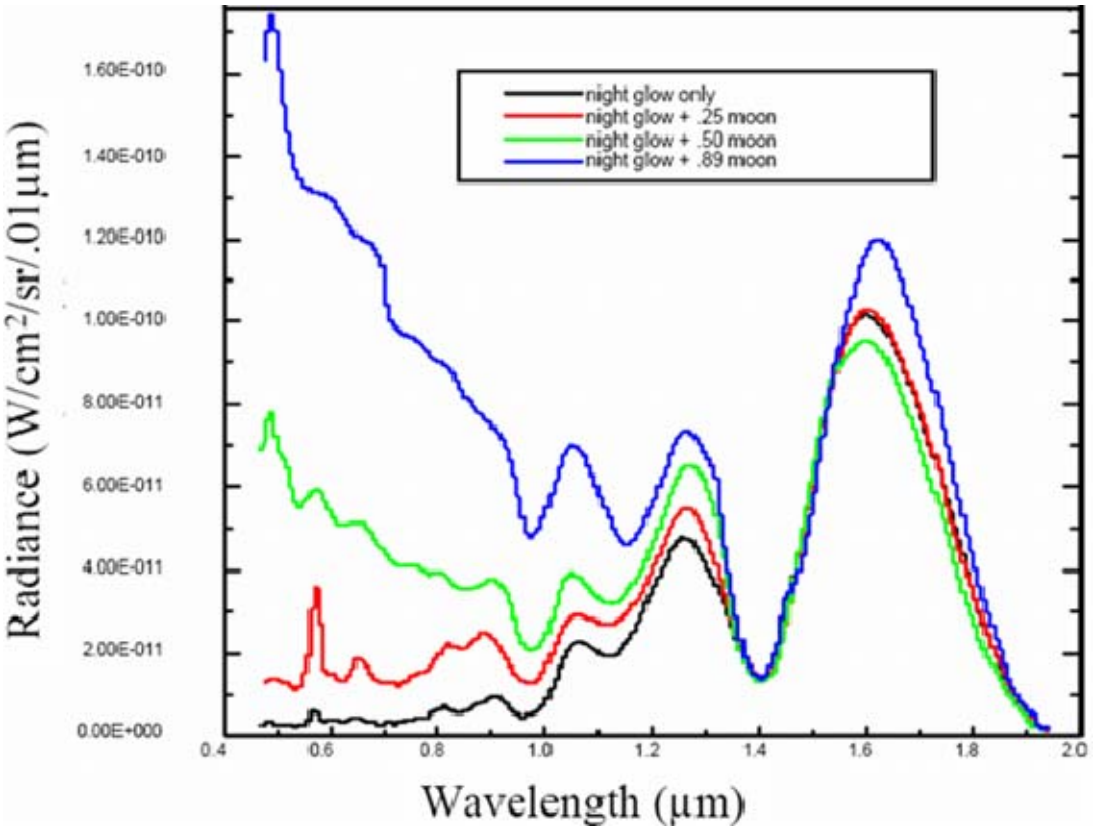

Figure 8. Radiance of Night Sky under different conditions (From [16])

With the increased use of eye-safe lasers, SWIR cameras are being integrated into current field goggles to image laser designator and rangefinder spots [17]. Figure 9 shows how SWIR images will be integrated with current field goggles to image laser designator and rangefinder spots.

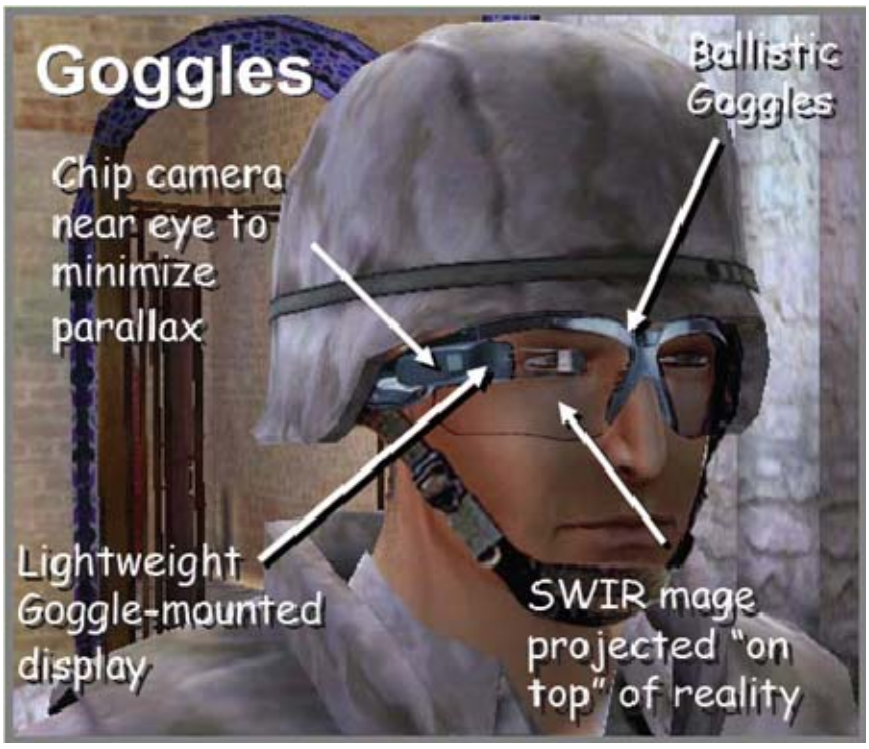

Figure 9. SWIR cameras are being integrated into current field goggles to image laser designator and rangefinder spots (From [17])

D. CAMOUFLAGE EFFECTIVENESS IN SWIR

While the U.S. military and allies continue to exploit the use of SWIR technology for enhanced imagery, one must be mindful that potential adversaries will eventually have similar programs that allow their soldiers to have enhanced imagery from various spectral regions. It is thus important to allocate time and research into the camouflage protection of soldiers and equipment in the SWIR spectral range. Current technologies in Counter-Camouflage, Concealment, and Deception (Counter-CC&D) do not consider the behavior of materials in the SWIR region. As a result, materials that effectively provide camouflage and concealment in the visible spectrum may not do so in the SWIR spectrum. This effect is best illustrated by comparing the two images in Figure 10.

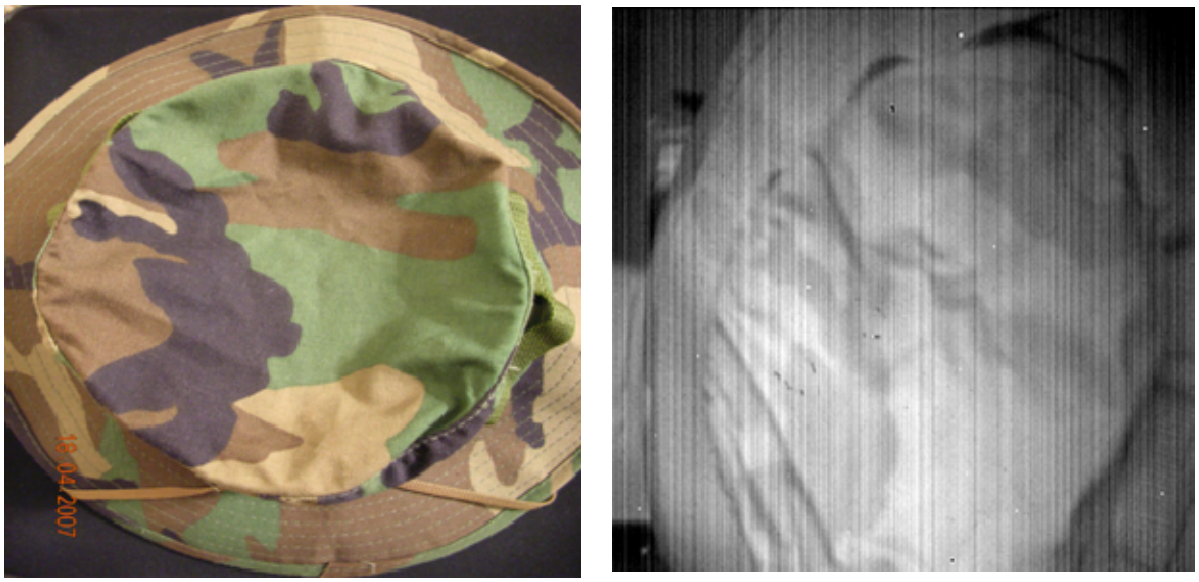

Figure 10. Image of camouflage hat taken using a Silicon CCD camera (left) and a SWIR camera in the 1.2 – 1.7 µm spectral region (right).

The visible patterns that were meant to camouflage soldiers operating in a woodlands environment “disappear” in the SWIR image. This is because the dyes of the fabric have different reflectivity of light in the visible spectrum. By reflecting different amount of visible light, camouflage patterns are presented to the human eye and any cameras operating in the visible spectrum. However, that is not the case in the SWIR region. All of the dyes used in this particular hat have similar reflectance of radiation in the SWIR. Hence the camouflage patterns are not apparent when presented to a camera sensing in the SWIR region and the hat appears not camouflaged.

The Marines and recently the Army have adopted digital or pixilated camouflage design for their new uniforms, namely the MARPAT and ARPAT. Advanced algorithms are used to generate the digital pattern. Micro-patterns are used to “decompose” the traditional macro-patterns into pixels that match the pitch size of a detector element in a focal plane array. This deteriorates the shape recognition ability of observers looking through imagers with a typical focal

plane array. A SWIR image taken of the Marine MARPAT hat, shown in Figure 11, exhibits a similar result when compared to the visible image. The patterns disappear, though to a lesser extent, compared to the previous version of woodlands camouflage.

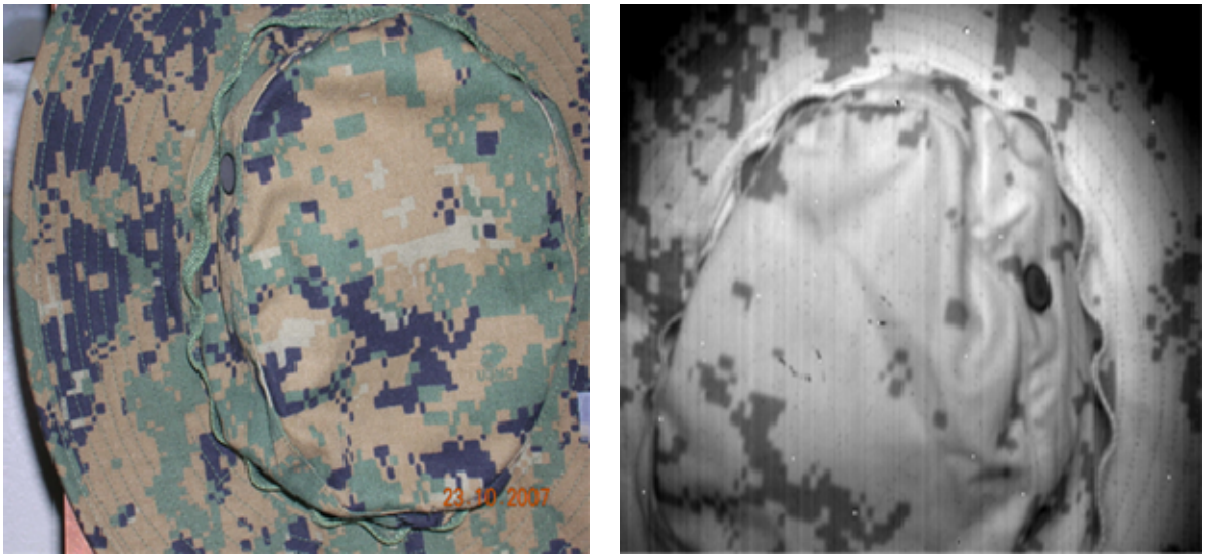

Figure 11. Image of MARPAT hat taken using a Silicon CCD camera (left) and a SWIR camera in the 1.2 – 1.7 µm spectral region (right).

Figure 12. shows a soldier standing in front of woodlands vegetation. The background consists mainly of leaves of high water content. Water absorbs radiation in the SWIR, specifically IR wavelengths at 1.4 and 2.5 µm, thus the vegetation appears dark in the picture. In contrast, the camouflage battle dress worn by the soldier reflects SWIR uniformly. Our soldiers donning these battle dresses are ineffectively camouflaged in the SWIR region.

Figure 13. presents an image of a Humvee in an urban environment. The camouflage pattern that is supposed to blend into the environment in the visible is less contrasting and less effective in the SWIR spectral region.

Figure 12. SWIR (0.9 – 1.7 µm) image of soldier against woodlands vegetation background (From [18])

Figure 13. SWIR (0.9 – 1.7 µm) image of a camouflage Humvee in an urban environment (From [19])

These results highlight the need for early research and development of camouflage material in the SWIR to enhance the protection of soldiers and equipment. Hence, the purpose of this thesis is to 1) develop a system for combined imagery and spectral reflectance measurements for the visible and SWIR regions (0.4 – 1.7 μm) to study the characteristics of materials in the SWIR spectrum and 2) to propose possible materials which effectively provide camouflage and concealment in the SWIR as well as the visible spectrum. The next chapter will describe the experimental set-up to study the reflectance of materials in the visible and SWIR spectral ranges.

THIS PAGE INTENTIONALLY LEFT BLANK

III. EXPERIMENTAL SET-UP

An experiment was designed to simultaneously study the reflectance characteristics and spatially image materials in the visible and SWIR spectrums. The experiment, conducted with the apparatus laid out on an optical bench as shown in Figure 14, was performed in an enclosed dark room. SWIR images are obtained with the capability for spatially resolved measure of reflectivity as a function of wavelength.

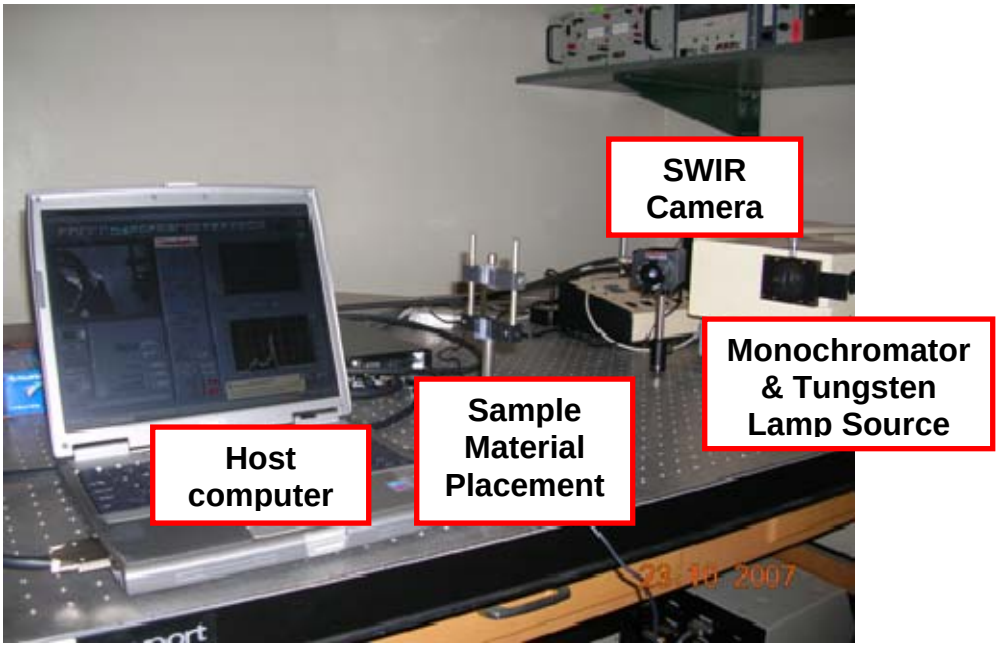

Figure 14. Optical bench with experimental apparatus

Essentially, the apparatus consists of a broad band light source coupled to a monochromator to direct light at a variable wavelength onto the sample material. The reflected light from the sample material is captured using a camera that has detection range in the visible as well as the SWIR, up to 1.7 μm. The image or video captured can be displayed on the host computer via a digital image acquisition board and subsequently processed, using an image

processing software and MATLAB, to determine the reflectance of the sample material as a function of wavelength. The next few sections will describe the equipment in detail and the experimental procedure.

A. MONOCHROMATOR

The PTI Monochromator Model 101, shown in Figure 15, coupled with a 100 W Tungsten-Halogen lamp provides the light source. The broad band light enters the 1/4-metre monochromator through the entrance slit and is diffracted from a 600 lines/mm ruled grating, with the blaze wavelength at 1 μm. The grating efficiency is shown in Figure 16.

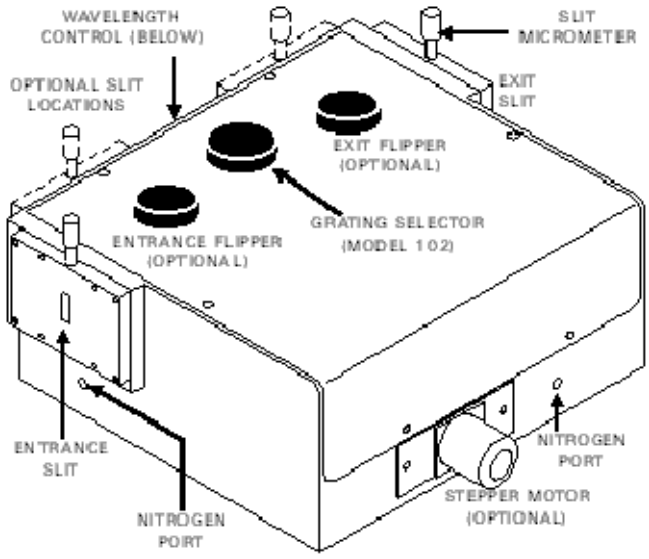

Figure 15. PTI Monochromator Model 101 (From [20])

This allows light at selected wavelength to be dispersed across the exit slit. The scanning range of the chosen grating covers the waveband of interest, i.e. 0.4 to 1.7 μm. A stepper motor is used to mechanically move the grating to produce light at selected wavelength and to achieve controlled scanning at various speeds.

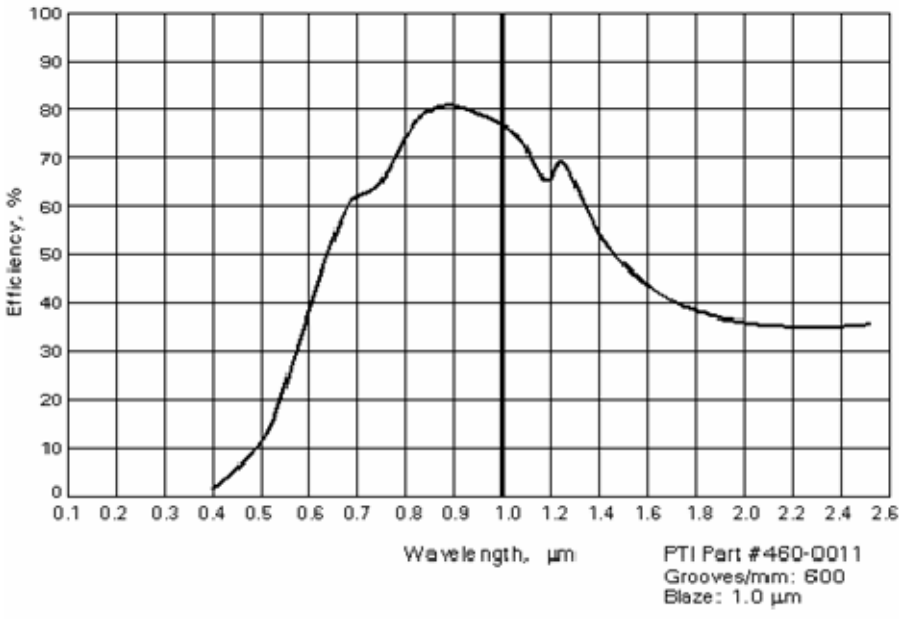

Figure 16. Grating Efficiency of the 600 lines/mm grating (From [20])

B. SWIR CAMERA - ALPHA™ NIR

Alpha™ NIR, a product of FLIR Systems – Indigo Operations, is used in the experiment to detect the reflected radiation from the sample material.

The Alpha™ NIR is a digital IR imaging sensor built using Visible Indium Gallium Arsenide (VisGaAs) photodetectors, arranged in a 320 by 256 pixel focal-plane array. The focal plane is indium bump bonded to a silicon Readout Integrated Circuit (ROIC). The camera is thermally stabilized or cooled by thermoelectric coolers to maintain the operating temperature around 20 ^{o}C. The camera is suitable for studying materials' characteristics in the visible and the SWIR because the detectors exhibits high spectral response from 0.4 to 1.7 µm as shown previously in Figure 4.

Figure 17. Alpha™ NIR, a product of FLIR Systems – Indigo Operations (From [10])

C. IMAGE PROCESSING USING IRVISTA & MATLAB

A standard C-mount lens is attached to the Alpha NIR for imaging applications. To acquire an image, the camera is connected to a host computer via the National Instruments™ digital image acquisition (IMAQ) board. The computer then controls the camera using the IRVista software. The software allows real-time image acquisition, storage, processing and analysis of images as well as video through a Windows interface.

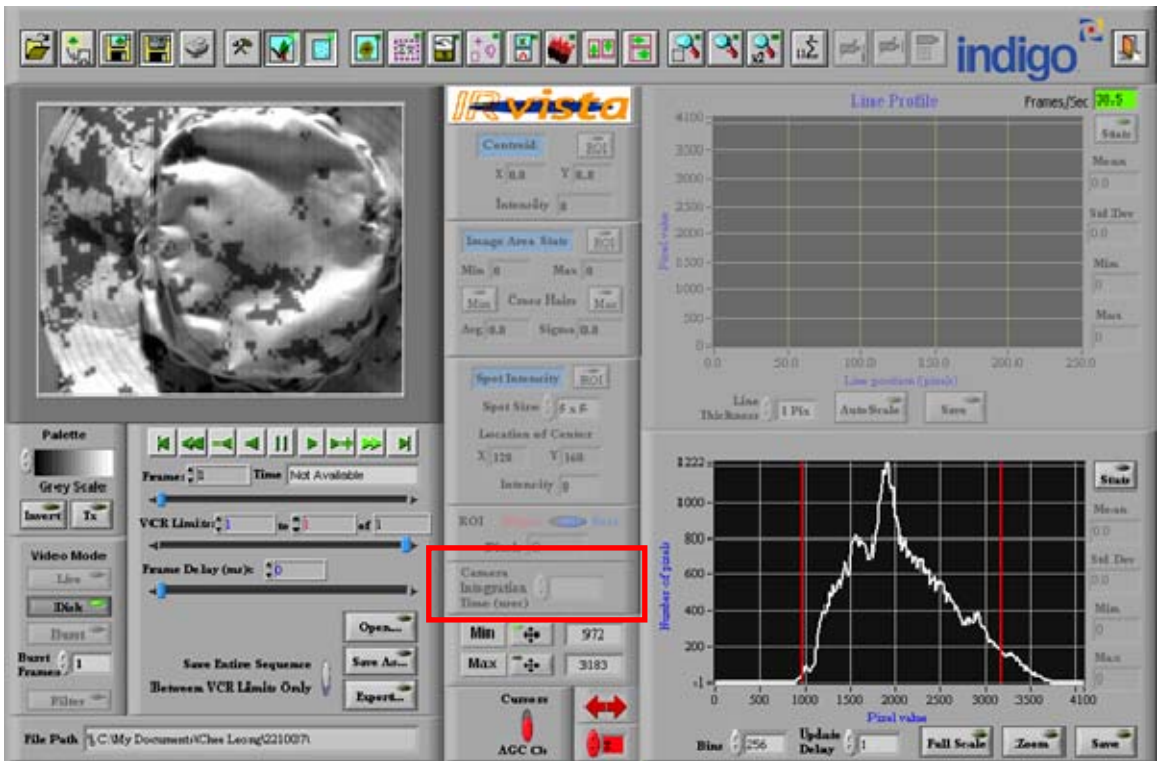

Figure 18. Front panel image of IR Vista™.

One important feature of the software is the flexibility in adjustment of the integration time per frame. The allowable integration times range from 25 microseconds to 33 milliseconds and from 35 milliseconds to 8.5 seconds, depending on the ambient light conditions. This feature is useful in that it allows capturing of high quality images under low light conditions, with the setting of a higher integration time. On the other hand, a lower integration time can be set when capturing images under bright or ambient conditions.

The camera produces 12-bit image data at a 30 Hz frame rate. IRVista captures the images in binary file format that are converted to 12-bit Tagged Image File Format (tiff), for ease of processing. The tiff file contains information on each frame in the form of a 320 by 256 matrix. The value of each element in the matrix represents the intensity registered by a corresponding pixel in the focal plane array, defined by its x and y coordinates. Table 1 shows a sample matrix of the 10 x 10 pixels sub-area of the image of the MARPAT hat shown in Figure 19.

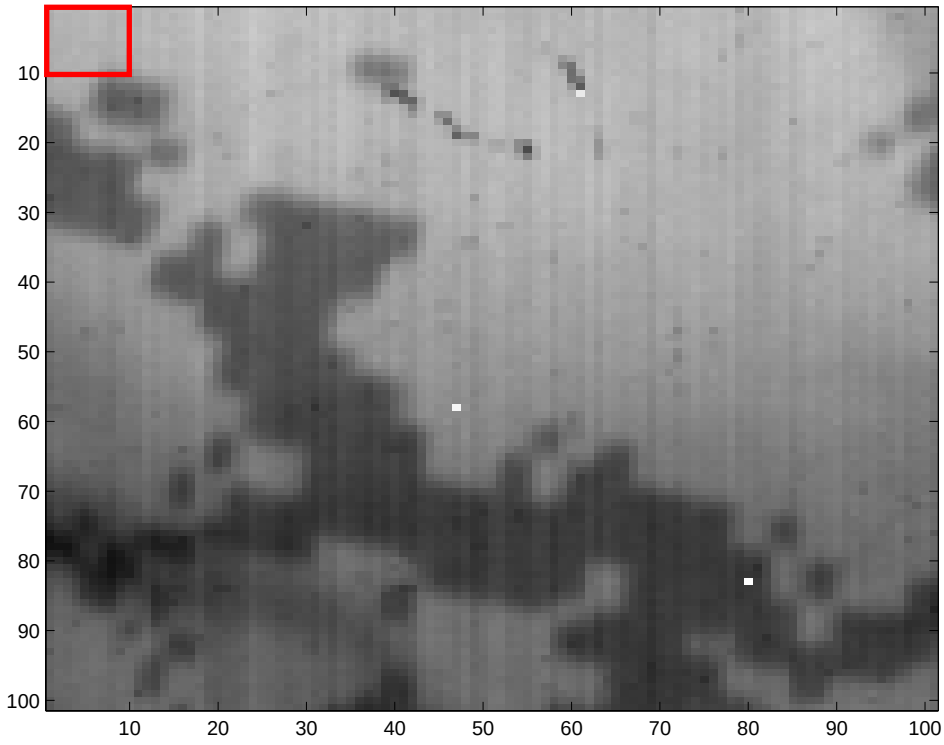

Figure 19. 2D Plot of 100 x 100 pixel sub-area of a MARPAT Hat

Pixel	1	2	3	4	5	6	7	8	9	10
1	174	186	182	183	187	193	185	177	187	189
2	170	184	183	183	187	188	183	177	183	187
3	175	184	183	181	183	187	184	180	185	187
4	171	180	179	182	180	184	182	177	180	183
5	174	181	178	181	180	185	183	175	181	182
6	173	178	178	179	178	184	180	175	183	184
7	173	176	175	179	180	183	181	176	183	184
8	175	175	175	179	176	175	176	175	178	182
9	171	173	176	182	176	179	174	175	180	178
10	173	175	179	176	178	180	174	171	176	173

Table 1. Matrix of 10 x 10 pixel sub-area of the MARPAT Hat

A stream of video can also be recorded in binary format. When exported to a tiff, it contains numerous matrices, 1 matrix for each frame recorded by in the

particular stream of video. MATLAB is a convenient programming language to manipulate the matrices. The 3D surface plot of the intensity of an area, such as the one shown in Figure 20, can be produced (refer to Appendix A for MATLAB codes for 2D and 3D plots).

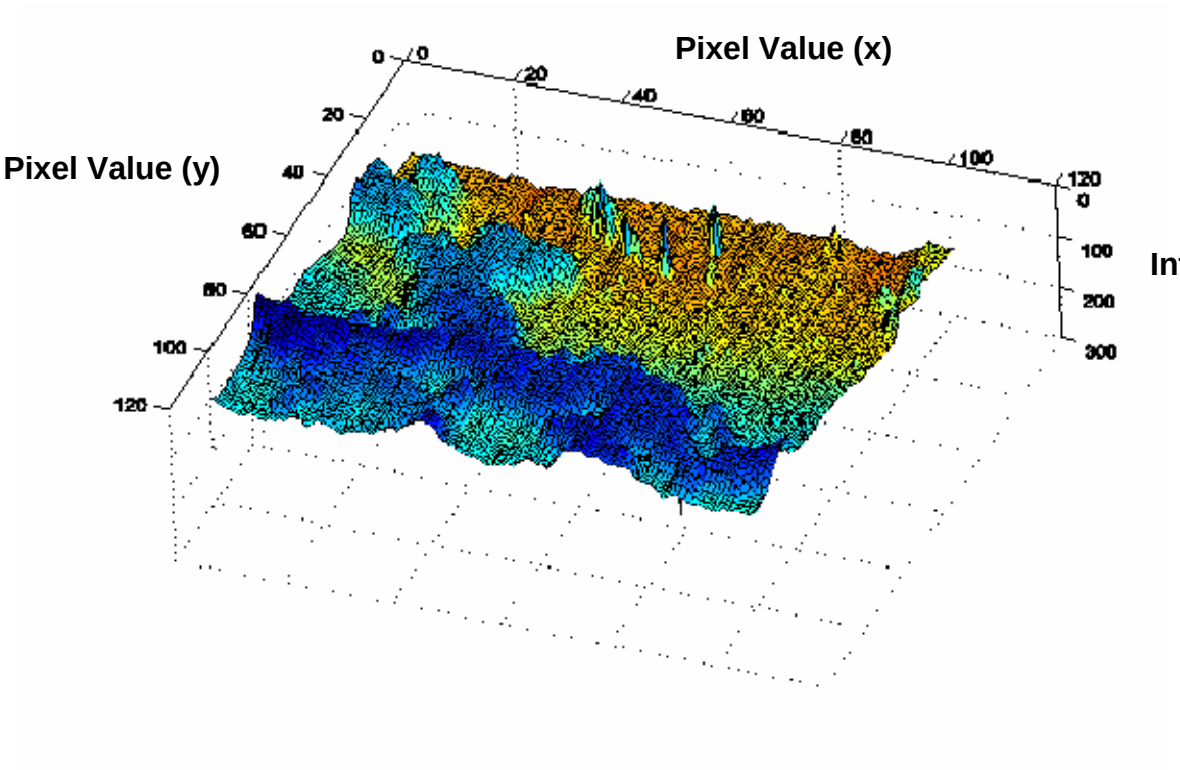

Figure 20. 3D surface plot of the MARPAT hat

This feature is useful for the study of the spatial variation of material reflectance over a range of wavelengths.

D. REFLECTANCE MEASUREMENT

The experimental procedure to measure materials' reflectance for visible and IR radiation is as follows. The stepper motor mechanically drives the grating such that the monochromator disperses light ranging from 400 to 1700 nm across the exit slit., at a rate of 2 nm per second. The light is reflected off the sample material and captured by the Alpha NIR camera, under dark room

condition to reduce background noise. A stream of video, consisting of a frame captured every 0.5 s, records the change in reflectance over time and wavelength.

The intensity of reflected light over an area on the sample at each time frame is determined from the tiff file using MATLAB. The intensity level such as those tabulated in Table 1 is the intensity of the signal read out from each of 100 x 100 pixels. MATLAB codes have been written to compute the average intensity. (refer to Appendix A for MATLAB codes) This average intensity is plotted over time to obtain the reflectance of a material as a function of wavelength.

A similar experiment was conducted to obtain the intensity distribution of the source. This time, the camera was directed towards the exit slit of the monochromator. The intensity over an average area within the light source is tabulated across a wavelength range of 400 to 1700 nm.

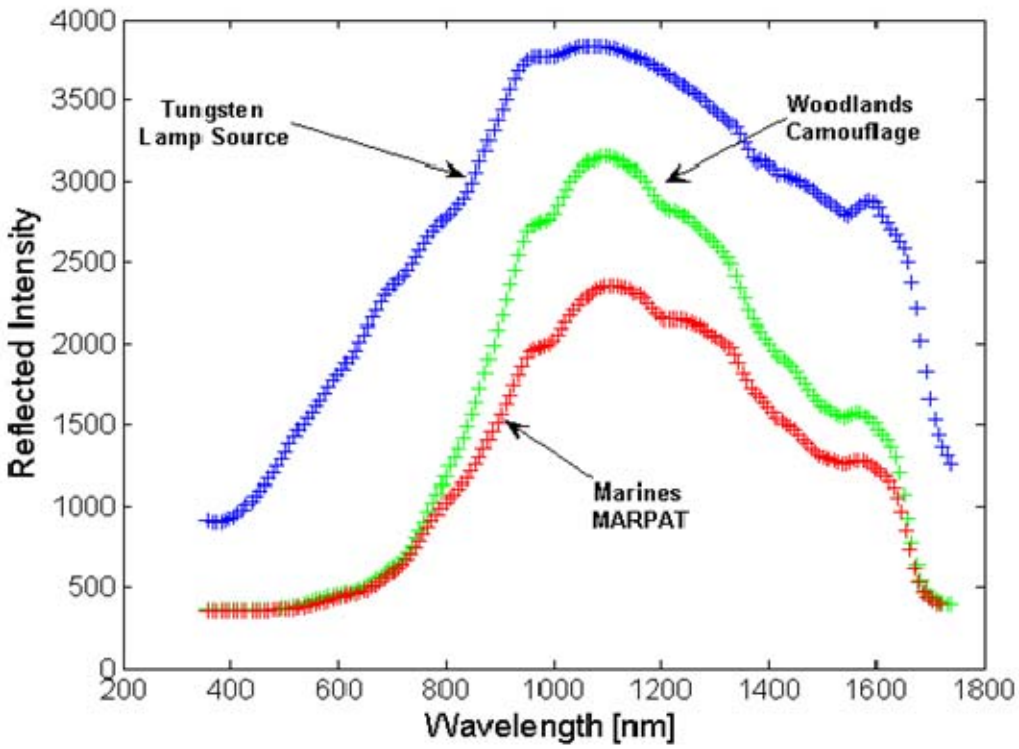

Figure 21. Plot of average intensity of the source and average reflected intensity from different camouflage materials as a function of wavelength.

Figure 21 shows the average intensity of the tungsten lamp source operating at 4 A and the average reflected intensity from sample areas of the woodlands camouflage and MARPAT hats.

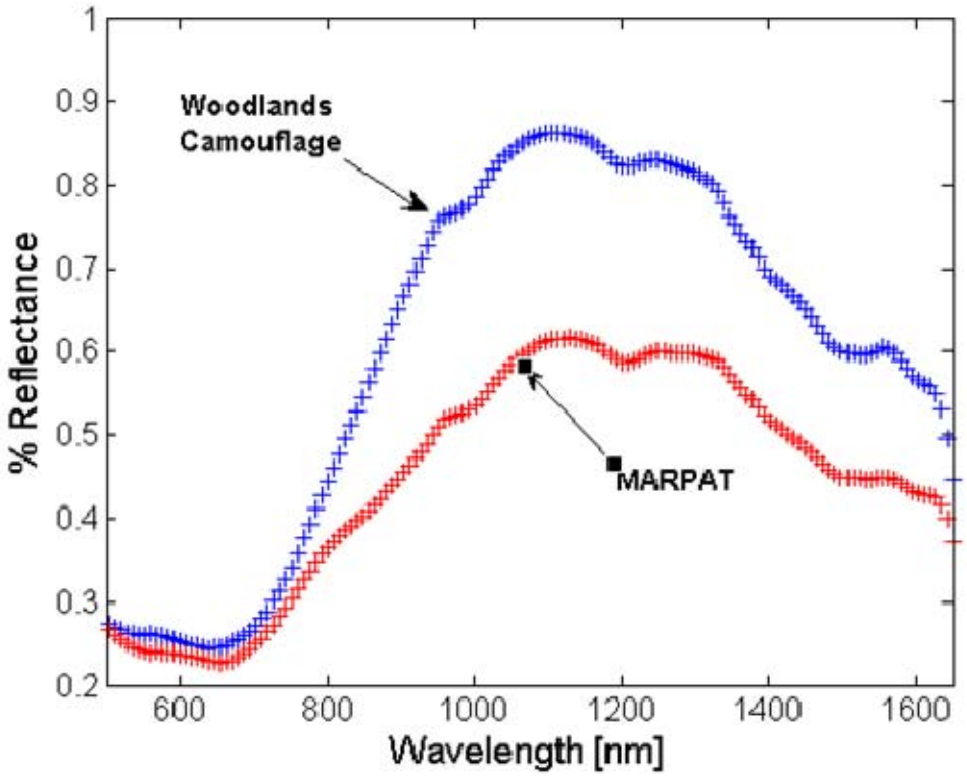

Figure 22. Plot of relative reflectance from different camouflage materials against wavelengths

Normalization is carried out to derive the relative reflectance. The normalized intensity is obtained using the average intensity divided by the intensity of the source at the particular wavelength. (refer to Appendix B for MATLAB codes to compute normalized reflectance) Figure 22 shows the normalized results for woodlands camouflage and MARPAT hats. The results show that both material exhibit significantly higher reflectivity in the SWIR as opposed to the visible part of the spectrum. This is probably because the materials have been designed to have reduced reflectance in the visible and NIR

spectrums, the spectral response range for NVDs. However, the designers of the camouflage material did not consider the reflectivity of the material in the SWIR.

In summary, an experimental set up with a combination of hardware and software was designed to study the characteristics of foliage as well as possible materials to provide effective camouflage in both the visible and SWIR spectrum. The results of experiments conducted on foliage and other materials are presented in the subsequent chapters.

IV. EFFECTIVE CAMOUFLAGE IN SWIR

Camouflage was first widely used during World War I to blend soldiers and other military equipment into their environment. However, the first use of camouflage can be traced back to 1857 when the British soldiers dyed parts of their uniform tan or khaki, in order to blend with the environment in India [21]. The first department set up in 1915 to design military camouflage for the French Army was headed by an artist. Since then, camouflage techniques have evolved from an art to a science. The design of camouflage has became increasingly challenging with the wide range of operating environments that soldiers can find themselves in, for a single operation.

Effective camouflage is usually achieved by reducing the optical contrast between the object and environment. Conventional camouflage textiles and paints use color and pattern to conceal the object from observers in the visible spectrum [22]. It has been shown that conventional camouflage textiles do not provide effective camouflage in the SWIR spectrum. Earlier developments of MWIR sensors brought about parallel research into textiles with controlled emissivity to manage the IR signature of soldiers. Similar research is necessary now to develop effective camouflage in the SWIR spectrum. A synopsis on camouflage techniques is presented in this chapter. This is followed by a discussion of the reflectance measurement of foliage in the SWIR. From the discussion on camouflage technique and foliage reflectance in SWIR, desired properties for materials that provide effective camouflage simultaneously in the visible and SWIR are proposed.

A. CAMOUFLAGE TECHNIQUE

Color, pattern and reflectance are widely recognized as important parameters for determining the effectiveness of camouflage design. Visible camouflage, used by military around the world to hide objects against woodlands background, consists of 4 common colors. Olive, khaki and light brown are used

to simulate positive space i.e. solid objects in nature such as rocks, soil and trees. Black is used to simulate negative or “empty” space in the environment. The camouflage pattern plays its part in reducing observers’ ability to make out the shape of the object against its background [21].

Modern digital camouflage design such as the U.S. Marine Corps pattern (MARPAT) incorporates micro-patterns to “decompose” the macro-patterns into pixels that matches the pitch size of a detector element in a focal plane array. This further deteriorates the shape recognition ability of observers looking through imagers with a typical focal plane array. In addition, the combination of the same visible camouflage colors is carefully chosen such that the overall percentage reflectance of the object is similar to that of negative space in the environment. This effectively camouflages the object by creating a false perception in the observer that he is looking into empty space when he is actually staring at the object. However, an initial experiment that measured the reflectance of MARPAT and common foliage highlights significant difference in reflectance of SWIR radiation.

B. FOLIAGE AND MARPAT REFLECTANCE IN THE SWIR

In this experiment, the reflected intensity from common foliage was taken over a range of wavelengths and normalized. The average reflectance of common foliage as a function of wavelength is as shown in Figure 23. There is significant reduction in reflectance around 1.4 μm.

This result is consistent with the results of an extensive study of the spectral reflectance by NASA Jet Propulsion Laboratory [23]. The spectral response of various material and vegetation as a function of wavelength is shown in Figure 24.

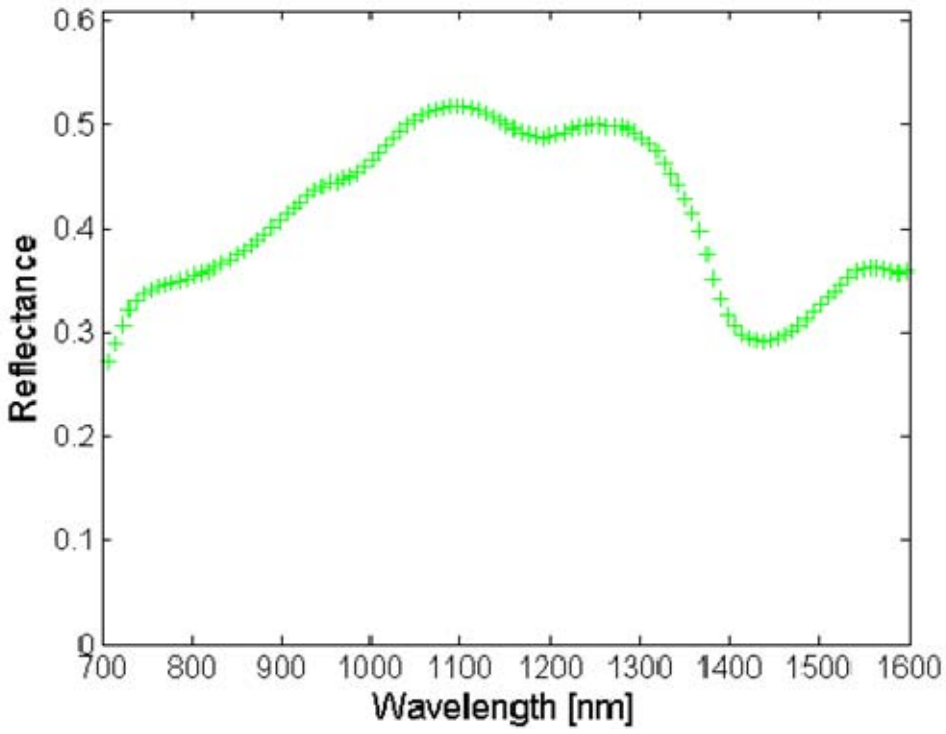

Figure 23. Average reflectance of common foliage as a function of wavelength

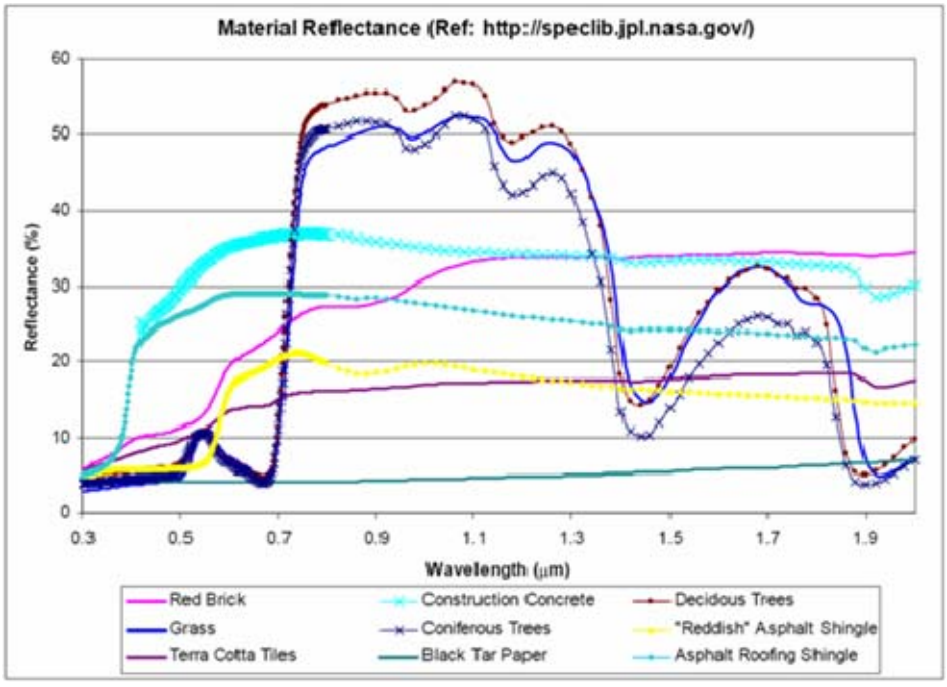

Figure 24. Spectral Response of various material and vegetation as a function of wavelength (From [23])

Trees and plants generally have low reflectance in the visible spectrum but the reflectance increases appreciably in the NIR and SWIR spectrum. The characteristic decrease in reflectance off foliage in the region of 1.4 μm is the result of strong absorption by water at that wavelength. The degree of reduction in reflectance varies with the amount of water content in the trees and plants. Results from an extensive study of the spectral reflectance of natural terrain elements show that the average reflectance off foliage across the visible and SWIR spectrum is generally lower during wet seasons.

The direct result of the significant difference in reflectance off foliage and MARPAT in the region of 1.4 μm is illustrated in Figure 25. The foliage in the background appears dark while the MARPAT appears white.

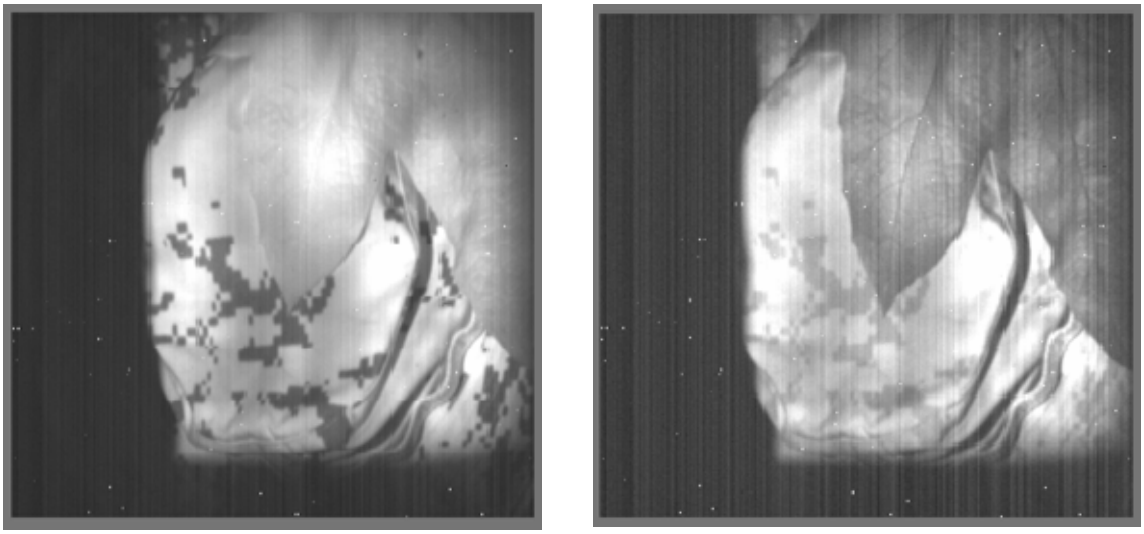

Figure 25. Image of a scene, with a leaf placed onto a MARPAT hat, taken using a SWIR camera under illumination of 0.9 μm (left picture) and 1.4 μm (right picture).

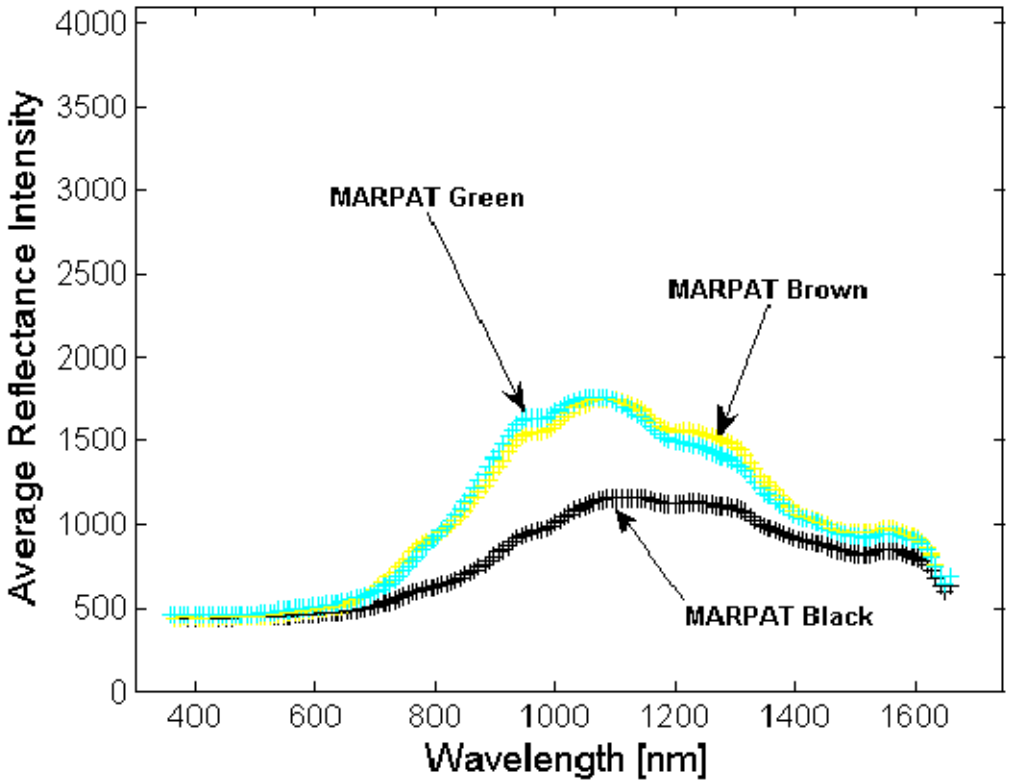

Figure 26. Average reflected intensity of various dyes in MARPAT hat as a function of wavelength

Figure 26 shows the minimal difference in reflectance of the green and brown colors of the MARPAT hat in the SWIR region. This result verifies the decrease in effectiveness of the camouflage because the camouflage pattern is not evident due to this lack of variation in their reflectance.

C. DESIRED PROPERTIES FOR CAMOUFLAGE IN VISIBLE AND SWIR

Color, pattern and reflectance are established as important parameters for determining the effectiveness of camouflage design. It has been shown that both the conventional camouflage textile and the MARPAT lack the ability to provide effective camouflage in the SWIR spectrum. The different color dyes exhibit different reflectivity of light in the visible spectrum. By reflecting different amount

of visible light, camouflage patterns are presented to the human eye and any cameras operating in the visible spectrum. However, these dyes have similar reflectance of radiation in the SWIR. Hence the camouflage patterns are not apparent when presented to a camera sensing in the SWIR region and the hat appears not camouflaged. There is also a significant difference in the average reflectance of SWIR off foliage and current camouflage textiles around the SWIR.

Therefore, a material must possess two desired properties to provide effective camouflage in the visible as well as the SWIR spectrum. First, the camouflage pattern must persist in the SWIR spectrum. This is achievable only if the contrast in reflectance, between each of the four dyes or paints, is consistent with their reflectance difference in the visible spectrum. Secondly, average reflectance of the material should be closely matched to that of the background across both spectral regions.

The next aim in this thesis is to consider modifications to existing textiles or the design of new camouflage materials that exhibit the two desired characteristics. The following chapter will describe how the reflectance of camouflage textile material can be modified by interlacing it with a layer of mesh.

V. REFLECTANCE TUNABLE MESH

Solar sailing is envisioned as a possible mechanism to power interstellar travel in the future. The basic idea is to have photons from the sun incident on a thin, light and reflective sail. Photons "bounce" off and transfer their momentum to a large sail, which in turn propels the space voyager [24].

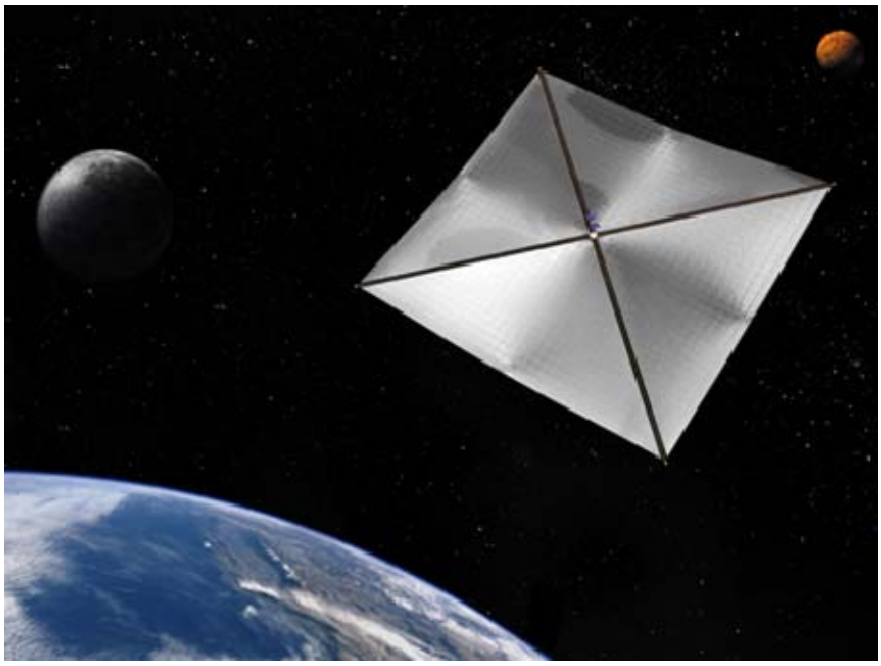

Figure 27. Artist's impression of a solar sail (From [25])

Photons possess a small amount of momentum ($p = E/c = h/\lambda$, where h is Planck's constant). Therefore, for this concept to work, it is essential to fabricate a sail that is extremely light and reflective. The use of a mesh as "perforated light sail" was proposed as a method to reduce the mass of the sail. A major consideration about the use of perforated mesh is that it must maintain its reflectivity despite being porous. The proposal led to detailed studies that derived

a relationship between reflectivity of a mesh and the spacing between the material that makes up the mesh. In another words, the reflectance of a mesh can be “tuned” by varying the mesh spacing.

More immediate application relevant to this thesis is the proposed reflectance tuning of camouflage materials using meshes. The contrast in reflectance between different color dyes of the fabric can be maintained in both the visible and SWIR spectrum by having layers of wearable nanomesh with different mesh spacing interlaced with conventional camouflage material.

A. MESH OPTICAL PROPERTIES

A theory of mesh optical properties was presented in a study on solar sails [24]. The mesh spectral fraction transmission, absorption and reflectance are derived for a typical mesh, as shown schematically in Figure 28.

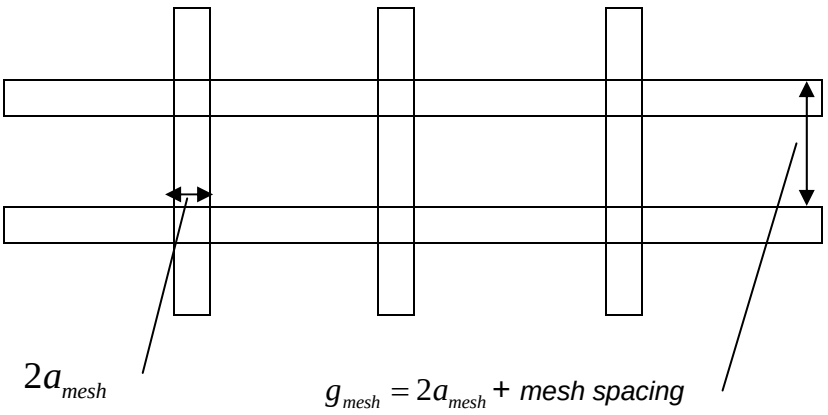

Figure 28. Perforated light sail constructed with mesh of rectangular wire

Key parameters are defined as follows:

- width of the mesh = $2a_{mesh}$,
- mesh parameter, $g_{mesh} = 2a_{mesh} + \textit{mesh spacing}$,

- thickness of the mesh = t_{mesh}
- cross-sectional circumference of mesh , $u_{mesh} = 8a_{mesh}$
- conductivity of the material, σ_{mesh}

The mesh spectral fraction transmission, $T_{\lambda,mesh}$, absorption, $A_{\lambda,mesh}$ and reflectance, $R_{\lambda,mesh}$, are derived under the following set of conditions.

- light wavelength, $\lambda >> 2g_{mesh} > 16a_{mesh}$
- $a_{mesh} > \delta$ (skin depth)
- $t_{mesh} < g_{mesh}$

$$T_{\lambda,mesh} \cong \frac{4g_{mesh}^2}{\lambda^2}\left\{ln\left[\sin\left(\frac{\pi a_{mesh}}{g_{mesh}}\right)\right]\right\}^2$$

$$A_{\lambda,mesh} \cong \frac{2g_{mesh}R_{\lambda,mesh}}{u_{mesh}}\left(\frac{c}{\sigma_{mesh}\lambda}\right)^{1/2}$$

From this, one can show that in the case of visible light incident on a mesh made up of aluminum mesh, the reflectance of a mesh would be primarily a function of the mesh spacing.

$\delta = 3$ nm (skin depth for visible light)

For $\lambda \approx 0.5\times10^{-6} m$, $\sigma_{mesh} \sim 3\times10^{17} s^{-1}$, $c = 3\times10^{8} ms^{-1}$,

$$\left(\frac{c}{\sigma_{mesh}\lambda}\right)^{1/2} \approx 0.045$$

And if $a_{mesh} = 10$ nm and mesh spacing = 50 nm,

$g_{mesh} = 70$ nm and $u_{mesh} = 8a_{mesh} = 80$ nm.

then, $A_{\lambda,mesh} \cong \frac{2g_{mesh}R_{\lambda,mesh}}{u_{mesh}}\left(\frac{c}{\sigma_{mesh}\lambda}\right)^{1/2} \cong \frac{2(70)R_{\lambda,mesh}}{80}(0.045) \cong 0.079R_{\lambda,mesh}$

Since $R_{\lambda,mesh} >> A_{\lambda,mesh}$, $T_{\lambda,mesh} \approx 1 - R_{\lambda,mesh}$

$$\therefore R_{\lambda,mesh} \approx 1 - \frac{4g_{mesh}^2}{\lambda^2}\left\{ln\left[\sin\left(\frac{\pi a_{mesh}}{g_{mesh}}\right)\right]\right\}^2$$

In another words, the reflectance of a mesh can be tuned by varying the mesh spacing or the fill factor (fraction of the mesh filled).

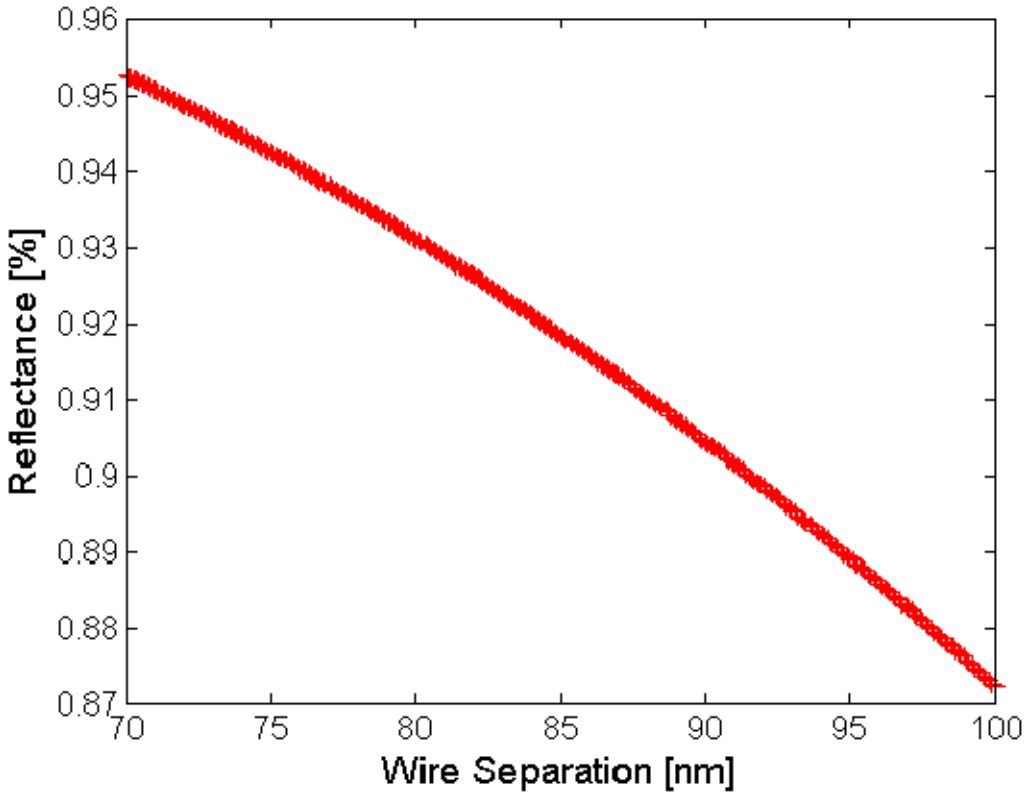

Figure 29. Reflectance as a function of mesh spacing for a 5 nm wire

To illustrate this, the reflectance of SWIR ($\lambda \approx 1200$ nm) off a mesh made up of 5 nm wire is computed for a range of mesh spacing and fill factor, using the expression derived above. Figure 29 shows the reflectance as a function of mesh spacing.

In this illustration, a_{mesh} is chosen to be 5 nm so that the condition $\lambda >> 2g_{mesh} > 16a_{mesh}$ can be satisfied. The results show that the reflectance can be varied by about 8% by varying the mesh spacing from 70 to 100 nm. Figure 30 shows the reflectance as a function of fill factor.

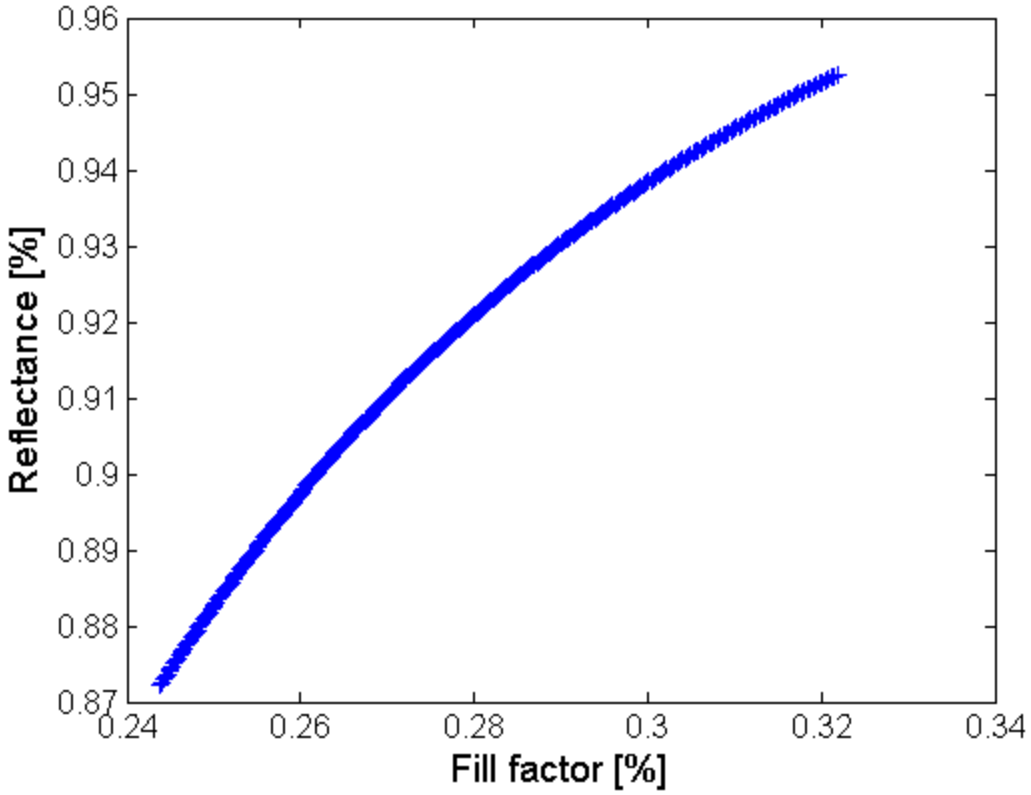

Figure 30. Reflectance as a function of Fill Factor for a 5 nm wire

B. REFLECTANCE TUNING TO ACHIEVE OPTICAL CONTRAST

There was little difference in the SWIR reflectance between the colored dyes of the MARPAT camouflage material. The results above suggest that a viable method to maintain contrast between color dyes is interlacing meshes of different spacing with the camouflage material with each dye.

Figure 31 shows the reflectance as a function of wavelength for 5 nm wire with 95, 70 and 50 nm mesh spacing. The average reflectance across the SWIR region is about 86.6%, for the mesh with 95 nm spacing. This mesh can be interlaced with the black camouflage textile.

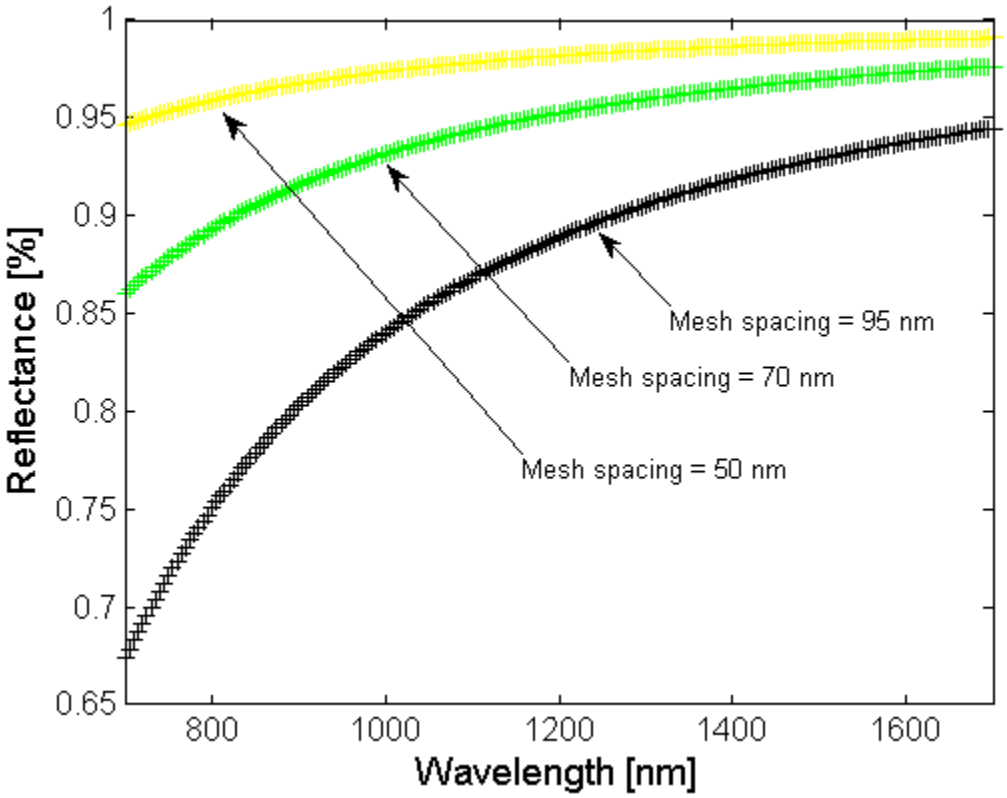

Figure 31. Reflectance as a function of wavelength for 5 nm wire with 95, 70 and 50 nm mesh spacing

When the spacing is decreased to 70 nm, the average reflectance across the SWIR region increases to about 94.3%. This mesh can be interlaced with the green camouflage textile. An average of about 8% difference in reflectance can be maintained between the green and black dye across the SWIR spectrum.

When the spacing is further decreased to 50 nm, the average reflectance across the SWIR region increases to 97.8%. This mesh can be interlaced with the khaki camouflage textile. This will maintain an average of about 4% difference in reflectance between the green and the khaki camouflage material across the SWIR spectrum.

C. EXPERIMENTAL RESULTS

The duration of this study would not allow the fabrication of nanomeshes with the desired optical properties. However, the concept of tuning the reflectance of material using meshes was verified using commercially available mesh. Figure 32 consists of two Scanning Electron Microscope (SEM) images of an aluminum mesh which has wires 30 µm thick with 2 µm spacing between the wires.

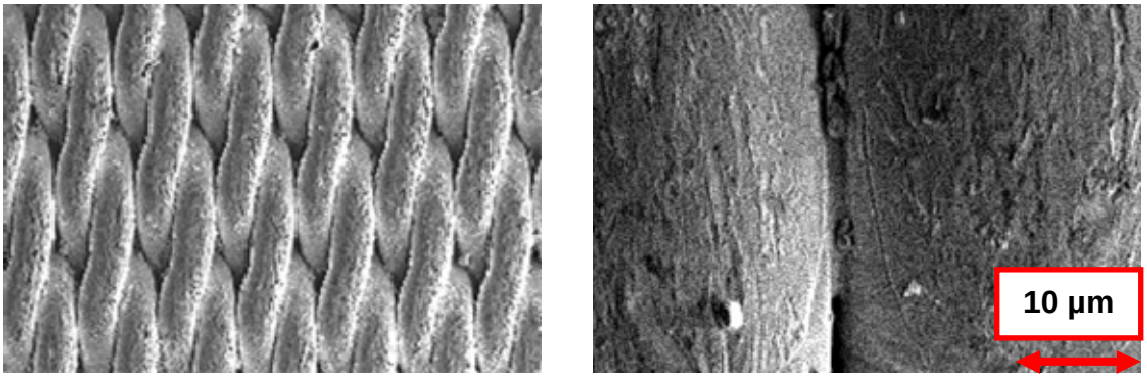

Figure 32. 250x magnification (left) and 2500x magnification (right) of an aluminum mesh with 2 µm mesh spacing, taken using a Scanning Electron Microscope (SEM)

Experiments were conducted to measure the reflectance of light off this mesh. The red curve in Figure 33 shows the normalized reflectance of visible and SWIR off a single ply of the mesh. Next, the fill factor is increased by overlapping two plys of mesh. The green curve in Figure 33 verifies an increase in reflectance with increase in the fill factor. The last experiment was to measure the reflectance off two plys of mesh orientated 45 degrees to each other. This time, the normalized reflectance significantly increased with the corresponding increase in the fill factor.

This mesh is not optimal for tuning the reflectance of visible and SWIR light because the condition, $\lambda >> 2g_{mesh}$, is not satisfied. However, the experimental results verify the relationship between reflectance and the fill factor.

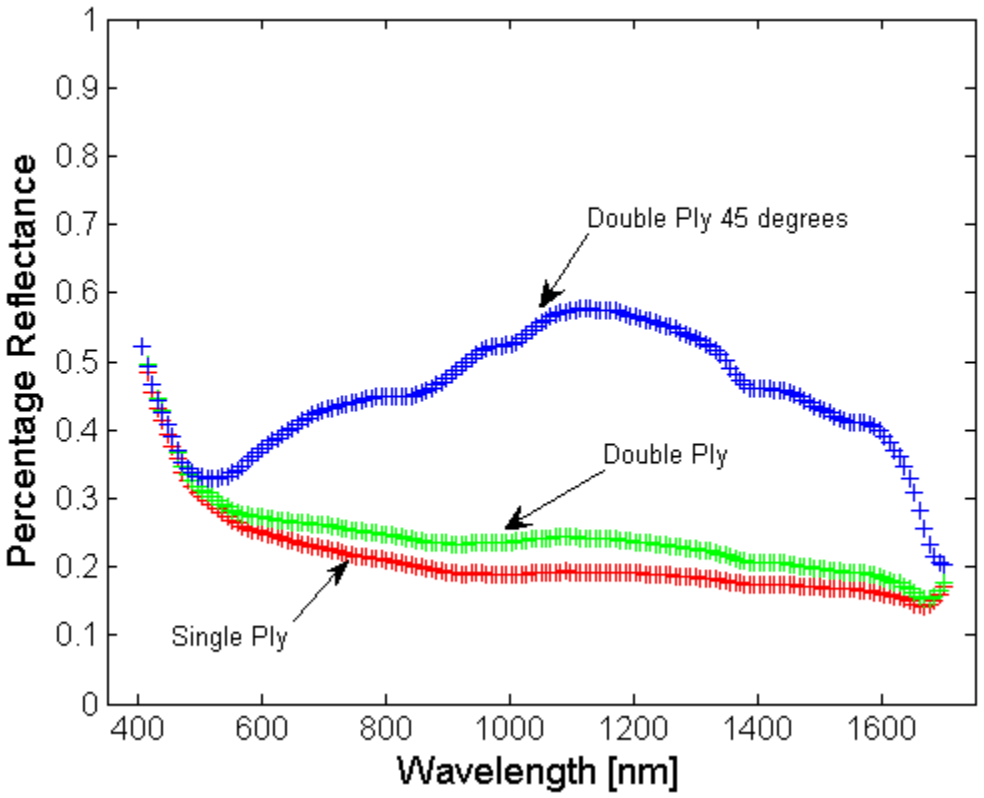

Figure 33. Reflectance as a function of wavelength for various configurations of meshes

In conclusion, current camouflage textiles can be interlaced with wearable nanomeshes to make the camouflage effective in both the visible and SWIR spectrums. Meshes of different spacing could be used to tune the reflectance of the material to maintain the contrast between different colors of the camouflage pattern. Furthermore, the overall reflectance of the material can potentially be tuned to a desired level that matches the reflectance of negative space in the environment.

The next chapter will describe how two different wavelength-tunable fibers can be used to further mimic the environment by creating an absorption-like behavior at 1.4 μm.

THIS PAGE INTENTIONALLY LEFT BLANK

VI. WAVELENGTH TUNABLE FIBER

Multi-spectral imaging can be used for the defeat of camouflage, concealment, and deception (CCD). The next section will describe how this can be achieved by comparing images of the same scene, taken in different spectral regions. Because foliage has different reflectance in the visible and the SWIR and a characteristic decrease in reflectance around 1.4 μm, digital imaging analysis techniques can be used to distinguish man-made objects from foliage in the scene [6].

The green color in camouflage material is used to replicate positive objects such as foliage in the environment. A mesh with the correct spacing could be chosen so that the modified camouflage material has comparable average reflectance with foliage across the SWIR spectrum. However, to further mimic the environment and avoid detection by multi-spectral imagers, the modified textile will have to exhibit the characteristic decrease in reflectance associated with water.

This could be achieved by “reinforcing” the new camouflage material with wavelength tunable fibers. One example of such wavelength tunable fibers has been produced by the group of Yoel Fink, an Associate Professor of Materials Science & Engineering at Massachusetts Institute of Technology (MIT) [26]. Fink and his team of researchers from various departments in MIT have produced fibers that have demonstrated the ability to be tuned to absorb radiation around a desired wavelength. Similar effects have been achieved using “chameleon” fibers, produced in the School of Materials Science & Engineering of Clemson University [27]. These fibers can potentially change colors and optical properties reversibly with structural changes to the chemical embedded within the fibers. This chapter will consist of a discussion on how these fibers can complement the combination of conventional camouflage material and wavelength-tunable meshes.

A. CAMOUFLAGE DEFEAT USING MULTI-SPECTRAL IMAGING

The Alpha NIR camera is well-suited for use as a multi-spectral imager because it operates in the visible, NIR and the SWIR spectrums. A full spectrum scene, consisting of a leaf placed on a MARPAT sample, is imaged at two different wavelengths, in a simple experiment to illustrate how multi-spectral imaging can be used to distinguish man-made objects from foliage.

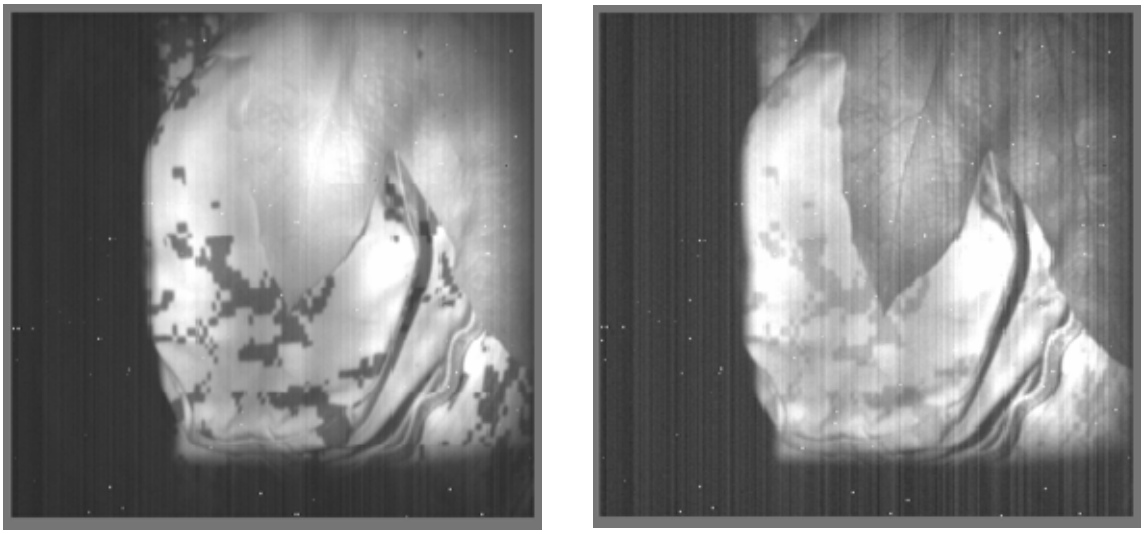

Figure 34. Images of a scene, with a leaf placed onto a MARPAT hat, taken using a SWIR camera under illumination of 0.7 μm (left picture) and 1.4 μm (right picture).

The left image in Figure 34 was taken under the illumination of 0.7 μm from the monochromator. A second image was captured under the illumination of 1.4 μm SWIR. The two matrices, containing the reflectance intensity of each pixels registered for each of the two images, were subtracted from one another. The resulting image, which is created by the contrast in reflectance between the two images, is shown in Figure 35.

The leaf can be clearly distinguished from the MARPAT hat because of its significantly lower reflectance in the SWIR spectrum due to strong water

absorption in the region of 1.4 µm. This is a useful counter-camouflage technique to detect military targets concealed by foliage in the back or foreground.

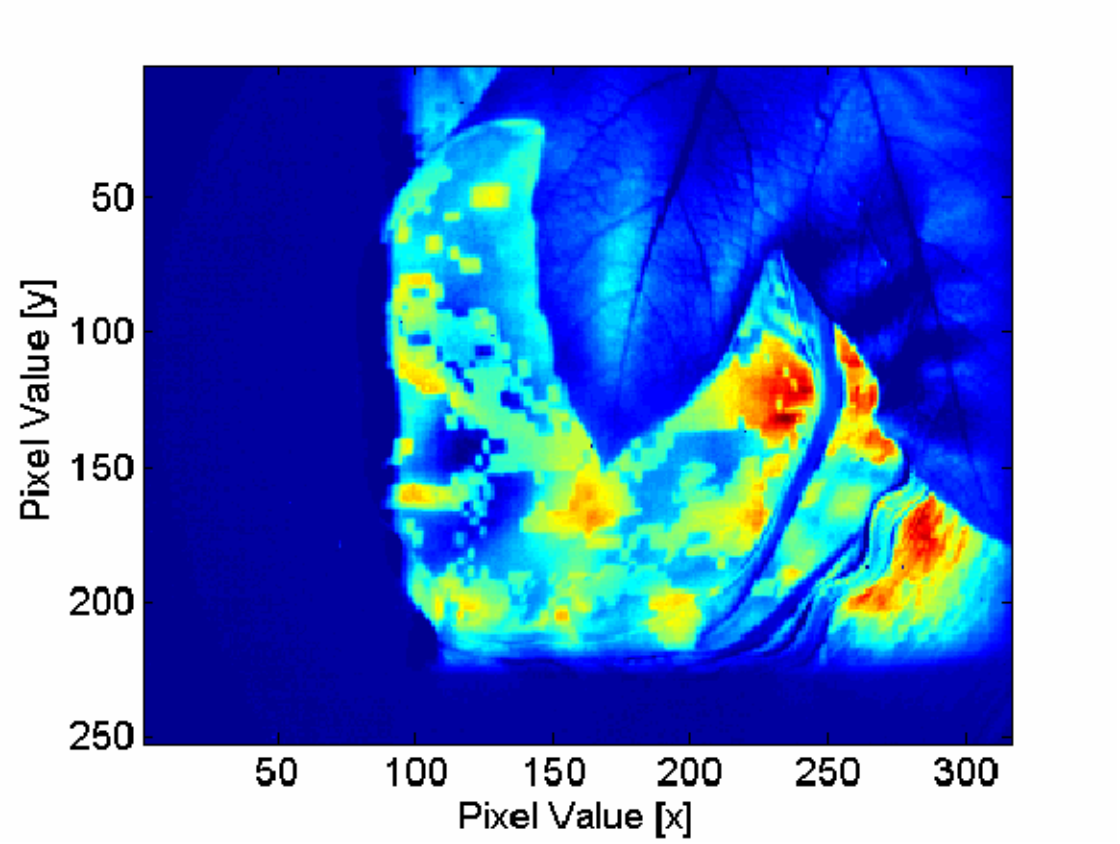

Figure 35. Image showing reflectance contrast between foliage and non-foliage objects by comparing visible and SWIR images.

B. OPTOELECTRONIC FIBERS

A new wavelength tunable fiber produced by Fink et al. [26] is a candidate material for smart uniforms in the future. When integrated in uniforms, the fiber serves as the detector material for lasers used in free-space communication. It could potentially also be used to reinforce the green dye in the new camouflage material, to mimic the behavior of foliage.

The optoelectronic fiber is made of a semiconductor (As-Se-Te-Sn) core contacted by metallic (Sn) electrodes and surrounded by a cylindrical-shell

resonant optical cavity. When the wavelength of the incident radiation matches the resonance wavelength of the cavity, the reflectance of the fiber is reduced because the light reaches the semiconductor core. The photons incident on the semiconductor core, which acts like a photodetector, generate a photocurrent in the metallic electrodes that run along the length of the fiber. This photocurrent can be detected when the electrodes are connected to an external circuit. Figure 36 shows a scanning electron microscope image of the fiber. Figure 36a is a micrograph of the cross-section of the fibre. The bright part of the fiber is the semiconductor core with four Sn electrodes attached. Figure 36b shows the resonant cavity structure. It consists of eight pairs of As_2Se_3/PEI multilayers, with a resonant cavity in the middle. Figure 36c shows the intimate contact between the semiconductor core and the Sn electrodes.

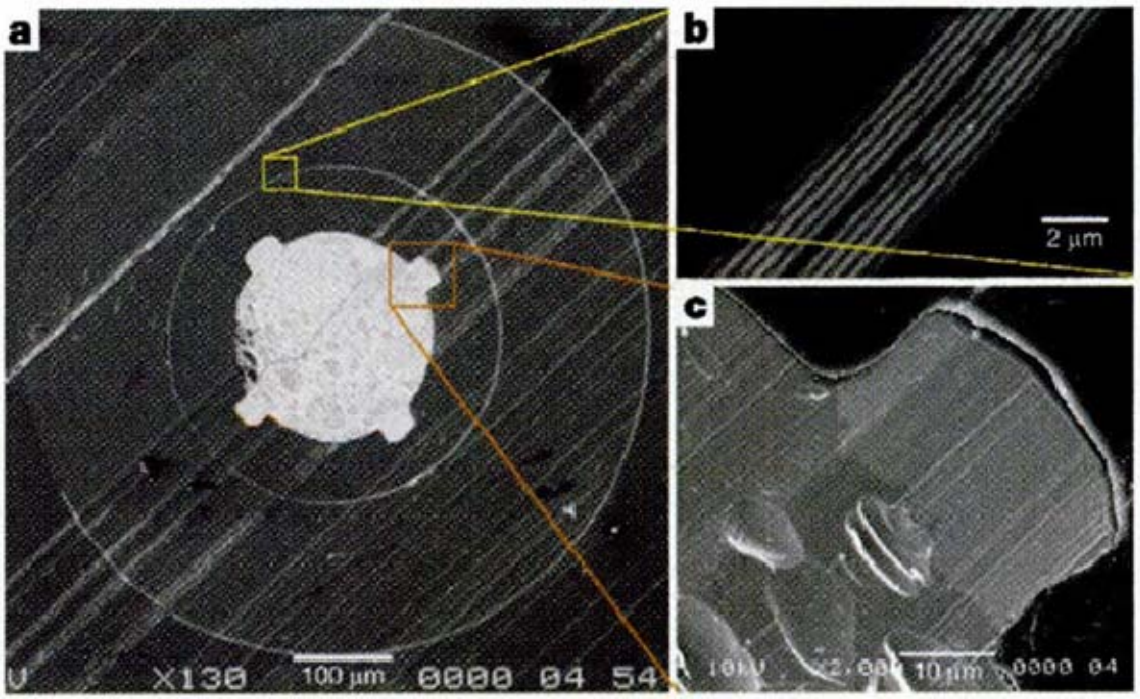

Figure 36. Scanning electron microscope image of the metal-insulator-semiconductor optoelectronic fiber (From [26]). Figure 36a is a micrograph of the cross-section of the fibre. Figure 36b shows the resonant cavity structure. Figure 36c shows the intimate contact between the semiconductor core and the Sn electrodes.

Figure 37 shows the reflectance and the generated photocurrent for such fibers with resonant wavelengths of 1.26, 1.29 and 1.33 μm respectively.

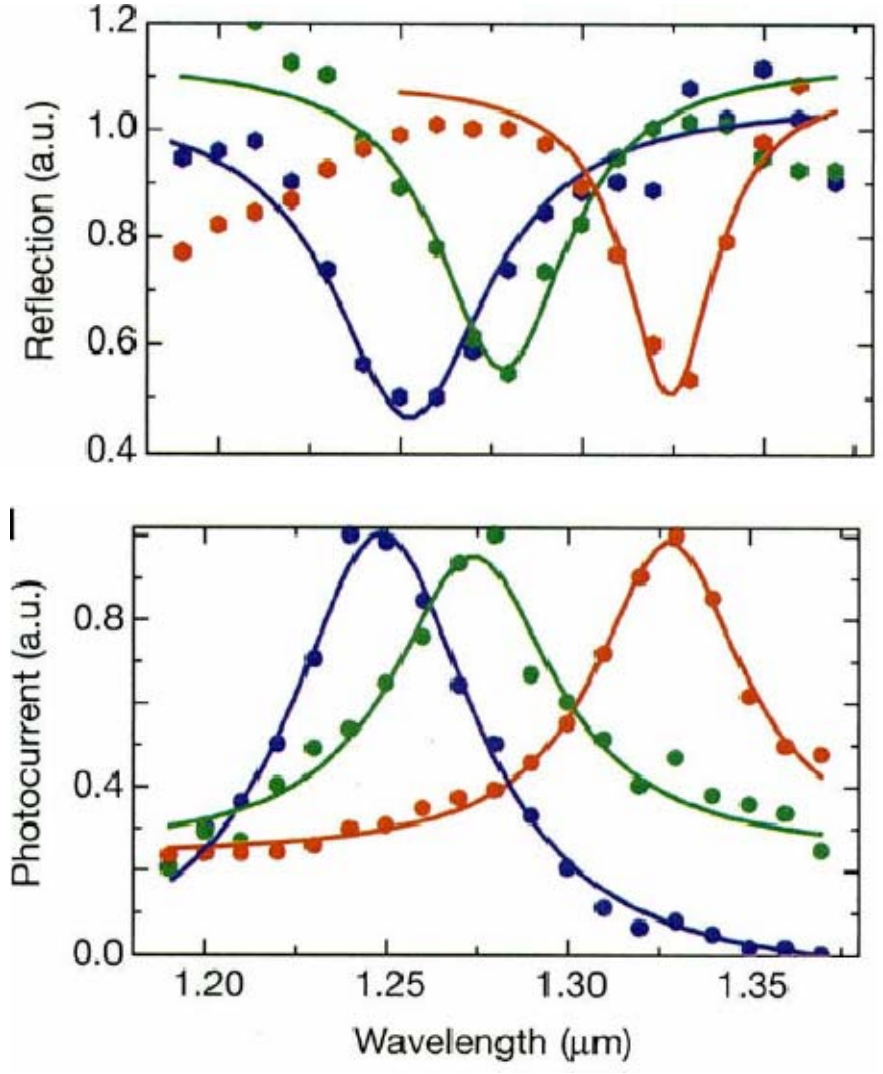

Figure 37. Reflectance measurements and photocurrents generated by fibers with resonant wavelengths of 1.26, 1.29 and 1.33 μm. (From [26])

The reduction in reflectance is observed over a range of wavelengths around the resonant wavelength, because the cavity resonance varies slightly with the angle of incidence of light. Therefore, the fiber originally manufactured to detect laser at specific wavelength can also be made to mimic the absorption of water if the fiber were tuned to absorb at a central wavelength of 1.4 μm.

C. REFLECTANCE MEASUREMENT OF OPTOELECTRONIC FIBER

This reflectance reduction around a resonant wavelength was verified in an experiment using fibers with cavity resonance designed for the visible part of the spectrum. Figure 38 shows a photograph of a sample tunable semiconductor fiber obtained from MIT.

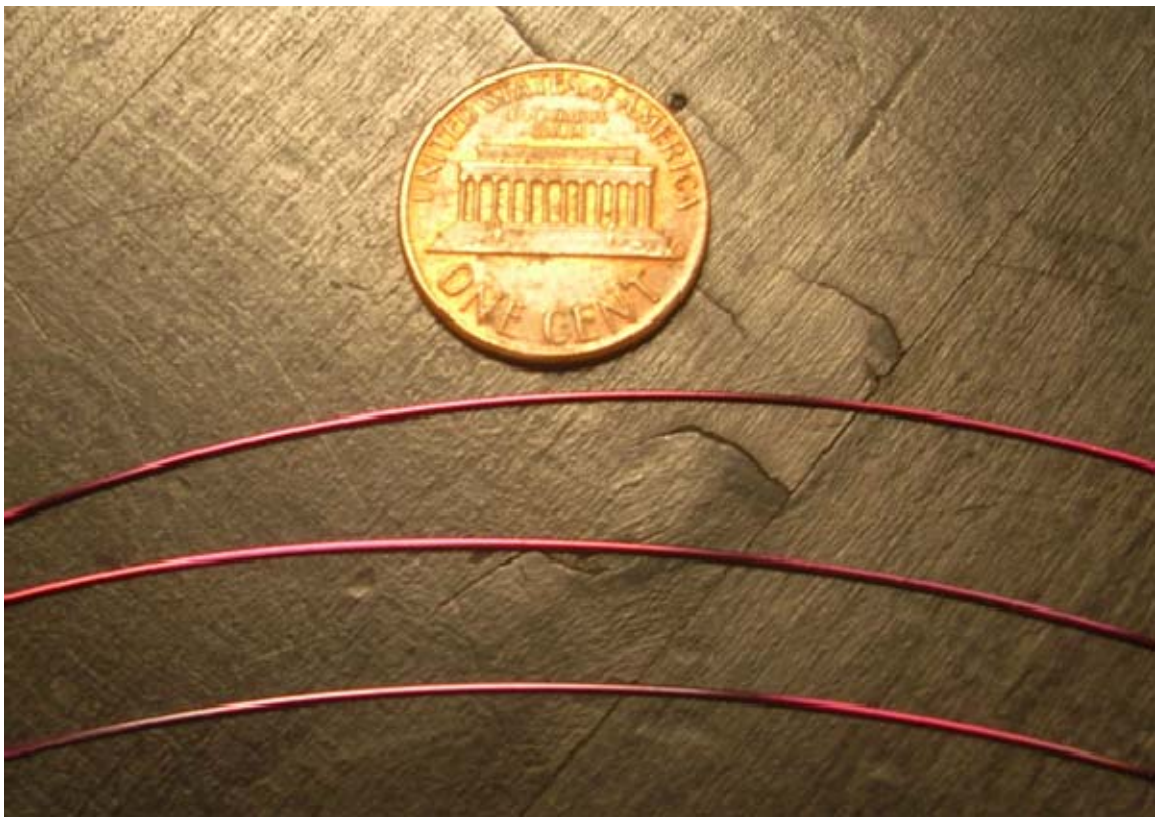

Figure 38. Optoelectronic fiber produced by MIT

The fibers shown in Figure 36 has the resonant cavity structure surrounded by cladding. The fibers in Figure 38 have resonant cavity structure on the outer surface of the fiber. They appear red because they have been tuned to absorb light around 0.55 μm. The reflectance of the fiber in the visible and NIR spectrum is measured using the system developed for reflectance measurements. Figure 39 shows significant reduction of reflectance around the

designed wavelength. The reason for the dip over a wider range of wavelengths is the wide range of angles from which light is incident on the fiber in our optical system.

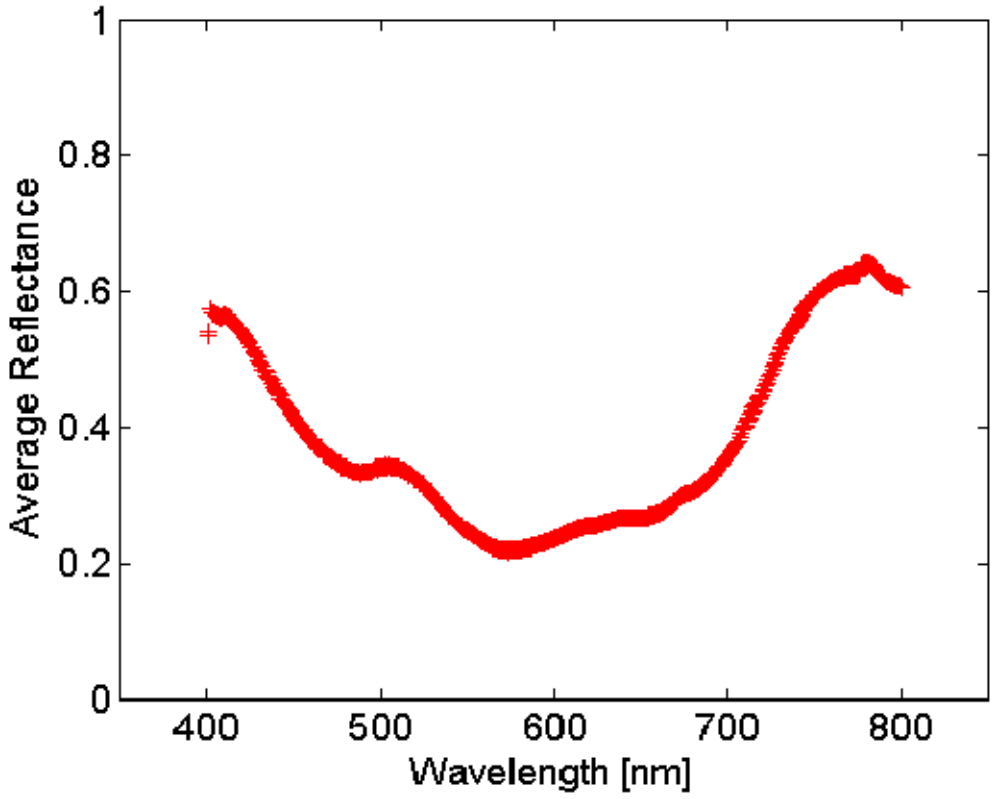

Figure 39. Reflectance measurement of the optoelectronic fiber from Figure 38

Hence the suggestion is to reinforce the new camouflage material with fibers tuned to absorb radiation around 1.4 μm region. That way, green fabric will exhibit similar reflectance as foliage across the visible and SWIR spectrum. The successful imitation of the characteristics absorption of radiation by water will deny multi-spectral imagers the ability to defeat the new camouflage material.

D. CHAMELEON FIBER

A similar effect could potentially be achieved using “chameleon” fibers – another approach to creating optically tunable response in fabrics [27]. As the name of the fiber suggests, soldiers donning uniforms made from these fibers are

effectively like chameleons. The color, shades and average reflectance of the uniform can be tuned to match the operating environment.

There are several approaches now under consideration for producing such color-changing fibers [28]. For example, electrochromism is a method to produce reversible and visible change in the absorption and reflection behavior of a material as a result of electrochemical oxidation and reduction. The fibers produced by the School of Materials and Science & Engineering of Clemson University, shown in Figure 40, change color because of structural changes to the chemical embedded within the fibers [29]. The fiber appears blue when the chemical is in its original state and appears red after structural change of the chemical occurs. The researchers in Clemson University claims that although the color change is permanent at this stage of the research, it can be made reversible in the near future.

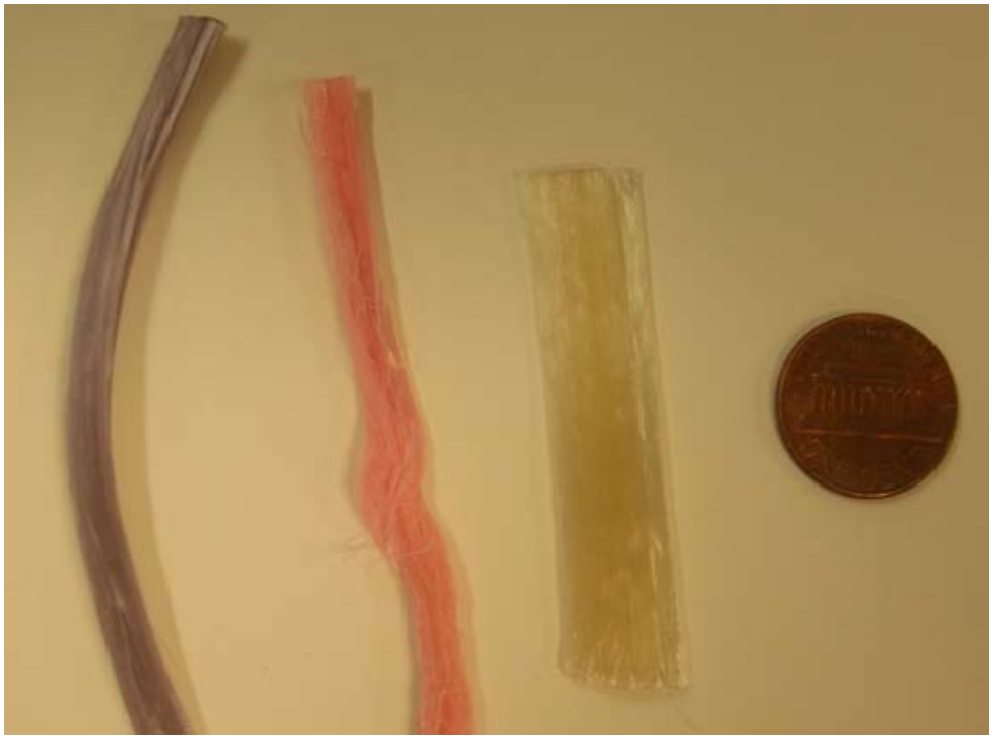

Figure 40. Bundles of chameleon fibers in their original blue color (left), fibers that appears red color (centre) after structural changes to the chemical & control fibers with no chemical embedded (right)

A reflectance measurement of the red fibers was taken using the system developed for spectroscopy. The reflectance from the fiber was divided by the reflectance from a control fiber with no chemical embedded. The ratio of reflectance from the red fiber is as shown in Figure 41. There is significant increase in reflectance around the 0.65 µm region.

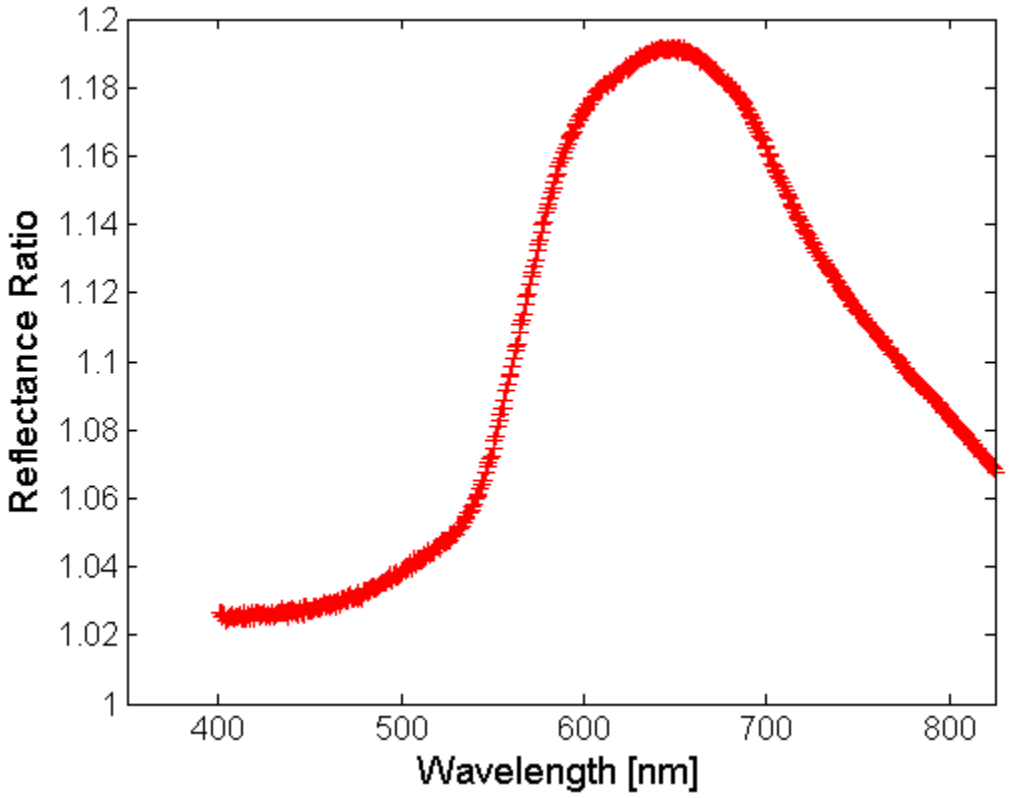

Figure 41. Reflectance ratio of the chameleon fiber from Figure 40

This ability to reversibly change optical properties and color presents many possibilities for camouflage applications. Reflectance contrast between the different color dyes in the SWIR can potentially be achieved by having the fibers, tuned to reflect at different wavelengths, reinforce the different color dyes. Figure 42 illustrates how reflectance contrast can be achieved if two fibers tuned to reflect around 1.2 and 1.6 µm respectively, are used to reinforce the brown and green dyes in the current camouflage material.

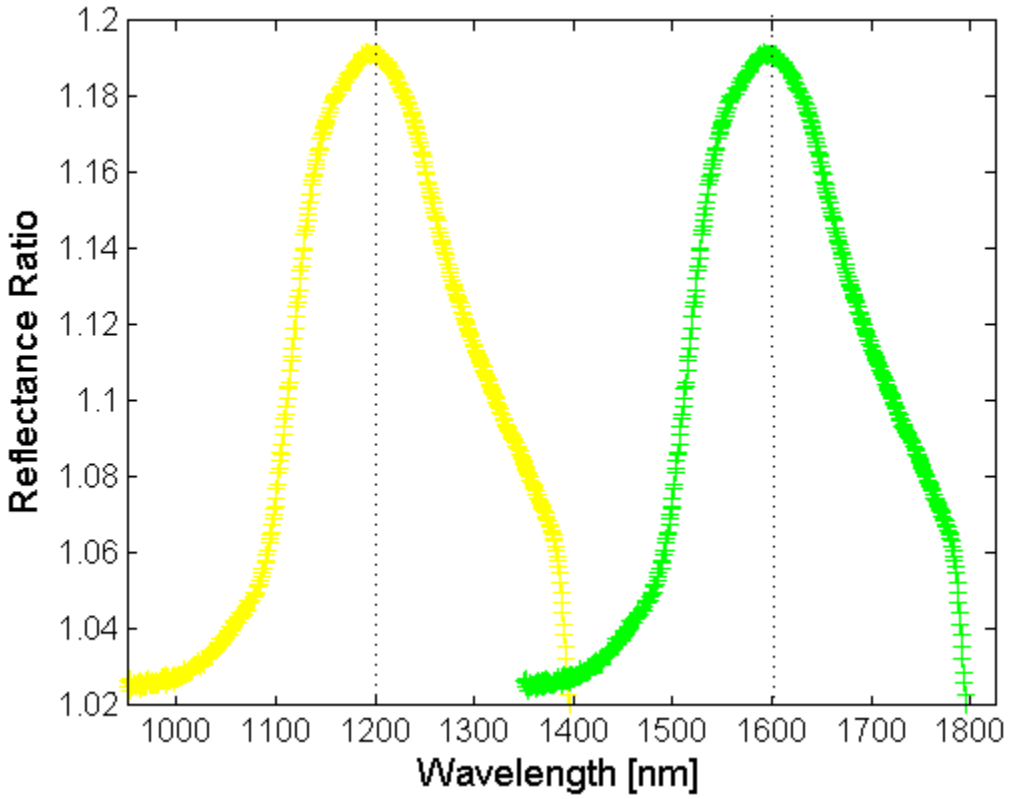

Figure 42. Simulated reflectance ratio of fibers tuned to reflect around 1.2 μm (left) and 1.6 μm (right) region.

Figure 42 also illustrates how foliage reflectance behavior can be mimicked using these fibers. By having two fibers' reflectance tuned to peak around 1.2 and 1.6 μm, appreciably decrease in average reflectance of the material can be observed around the 1.4 μm region.

In summary, the wavelength tunable fibers and chameleon fibers are two possible ways to ensure effective camouflage against multi-spectral imagers. They can be used mimic the environment by absorbing or reflecting at tunable wavelengths.

VII. CONCLUSIONS

A. SUMMARY AND CONCLUSIONS

In the evolution of weapons, the invention of a sharper sword has always brought about the invention of a stronger shield [30]. To defeat multi-spectral sensors or even image intensifiers with extended spectral response in the SWIR, effective camouflage that works in both the visible and SWIR spectrum is required. The aim of this thesis is to propose means to provide effective camouflage in both the spectral regions.

The first step towards achieving the aim was to develop a system for combined imagery and spectral reflectance measurements in the visible and the SWIR regions. The system was used to conduct experiments to study the reflectance of materials in both spectrums. From these experiments, it was ascertained that a material must possess two desired properties for it to provide effective camouflage in the visible as well as the SWIR spectrum. First, the contrast in reflectance between each of the dyes would have to be maintained throughout the entire spectrum of interest, in order for the camouflage pattern to persist. Secondly, the average reflectance of the material should be closely matched to that of the background, in both spectral regions.

Initial studies and experimental results show that nanomeshes are suitable as complement to current camouflage materials because reflectance of meshes varies with parameters such as the mesh spacing. Thus, the overall reflectance of camouflage materials can be tuned and the contrast between different dyes can be maintained by having meshes with different reflectance interlaced with conventional camouflage textile.

To further mimic the environment and deny detection by multi-spectral sensors, it is recommended that the meshes and fabric be reinforced by

wavelength tunable fibers. These fibers tuned to absorb in the region of 1.4 μm replicate the strong water absorption, a characteristic behavior of foliage in the SWIR.

In conclusion, it is proposed that the conventional fabric be reinforced with nanomeshes and wavelength tunable fibers, in order to defeat multi-spectral imagers by providing more effective camouflage in the visible and SWIR spectrums.

B. SUGGESTIONS FOR FUTURE RESEARCH

In the course of this study, experiments were conducted on commercially available micronmeshes. While the experiment verifies the relationship between reflectance and the fill factor, the mesh does not meet the criteria required to effectively tune reflectance of visible and SWIR radiation. Therefore, the first recommendation would be to fabricate nanomeshes with the actual dimensions required for tuning the reflectance of visible and SWIR radiation, once the technology to manufacture them matures. The new material will have to be reinforced with fibers custom-made to absorb around 1.4 μm. This will enable experiments to measure the reflectance of camouflage materials complemented with these meshes and fibers. The effectiveness of the camouflage material for visible and SWIR can thus be verified.

The next step would to conduct trials in simulated field environment such as the Camouflage Evaluation Facility in the Natick U.S. Army Soldier Systems Center, before actually mass producing the new camouflage materials and conducting field trials to verify the effectiveness of these new camouflage material.

Finally, studies should be conducted on the thermal emissivity of the new camouflage material. Materials that exhibit desired reflectance in visible and SWIR with controlled thermal signature in the MWIR and LWIR would be the complete solution to defeat multi-spectral imagers.

APPENDIX A. MATLAB CODES TO PRODUCE 2D, 3D SURFACE PLOTS AND TO COMPUTE AVERAGE REFLECTANCE AS A FUNCTION OF WAVELENGTH

```
clear;

for i=1:174

%To create a matrix of intensities registered by the pixels over an area
of interest specified by the values in square parentheses.

intensity = imread('MARPAT860.tif','PixelRegion',{[10 110],
[60 160]},i);
intensity = double(intensity);

%To create a 2D plot of the area specified above
figure(1);
imagesc(intensity);

Wavelength = 350+i*(1400/174);
string=int2str(Wavelength);
text(0,175,string);

xlabel('X-direction [Pixel No.]');
ylabel('Y-direction [Pixel No.]');
title('Surface Plot of at Specific Wavelength');

%To create a 3D surface plot of the area specified above
figure(2);
surf(intensity);

axis([0, 210, 0, 210, 0,4200]);
view([-2,-10,-40]);

xlabel('X-direction [Pixel No.]');
ylabel('Y-direction [Pixel No.]');
zlabel('Intensity');

%To compute and plot the average intensity as a function of wavelength
figure(3);
Avg = sum(intensity(:))/numel(intensity);
Vector(i) = Avg;
Wavelength = 350+i*(1400/174);
plot(Wavelength,Avg,'B+');
axis([300, 1750, 0,4100]);
xlabel('Wavelength [nm]');
ylabel('Average Intensity');
title('Plot of Average Reflectance Intensity over Area at Specific
Wavelength');
hold on;

end
```

THIS PAGE INTENTIONALLY LEFT BLANK

APPENDIX B. MATLAB CODES TO COMPUTE NORMALIZED REFLECTANCE AS A FUNCTION OF WAVELENGTH

```
clear;

for i=1:165

%To create a matrix of intensities registered by the pixels over an area
of Tungsten source specified by the values in square parentheses.

intensity = imread('Tungsten12.tif','PixelRegion',{[50 150],
[125 225]},i);
Avg = sum(intensity(:))/numel(intensity);
Vector(i) = Avg;

Stop = 830;
Wavelength = 350+i*((2*Stop-350)/165);

%To create a matrix of intensities registered by the pixels over an area
of the Woodlands Camouflage Hat specified by the values in square
parentheses.

intensity1 = imread('Leaf830.tif','PixelRegion',{[50 100],
[150 200]},i);
intensity1 = double(intensity1);
Avg1 = sum(intensity1(:))/numel(intensity1);

%To compute and plot the normalized reflectance as a function of
wavelength.

Vector1(i) = Avg1/Avg;
plot(Wavelength,Vector1(i),'G+');

axis([300, 1750, 0,1]);
xlabel('Wavelength [nm]');
ylabel('% Reflectance');
title('Plot of % Reflectance over Area at Specific Wavelength');
hold on;

end
```

THIS PAGE INTENTIONALLY LEFT BLANK

LIST OF REFERENCES

[1] Jeffery Paul. “MANTIS Program Update.” Soldier Technology U.S. 2007 Conference. June 2007.

[2] Electro Optical Industries Inc. “Atomspheric Transmission.” http://www.electro-optical.com/bb_rad/atmo_abs.htm (last accessed December 6, 2007).

[3] Ronald G. Driggers, Paul Cox and Timothy Edwards. “Introduction to Infrared and Electro-optical Systems.” Boston: Artech House Publishers, 1999.

[4] Martin H. Ettenberg and Doug Malchow. “Shortwave Infrared (SWIR) Imaging Aids Laser Tracking, Detection.” Photonics Tech Briefs April 2007. 24 May 2007. http://www.ptbmagazine.com/features/2007/feat2_0407.html (last accessed December 6, 2007)

[5] Matthew Kalman. “Hezbollah night-vision gear was from Britain.” San Francisco Chronicle on the We,b 20 August 2006. http://www.sfgate.com/cgi-bin/article.cgi?file=/c/a/2006/08/20/MNGK9KLVH41.DTL (last accessed December 6 2007).

[6] Stephen A. Drury. “Image Interpretation in Geology.” Oxford: Routledge, 2001.

[7] Devon C. Nugent. “Analysis of Foveon Multi-spectral Images for Counter-Camouflage, Concealment and Deception Application.” Thesis: Naval Postgraduate School, 2005.

[8] Richard C.Shirkey and Melanie Gouveia. “Weather-Impact Decision Aids: Software to Help Plan Optimal Sensor and System Performance.” The Journal of Defense Software engineering December 2002. 22 May 2007. http://www.stsc.hill.af.mil/crossTalk/2002/12/shirkey.html (last accessed December 6 2007).

[9] Sensors Unlimited. “Technology: What is InGaAs.” http://www.sensorsinc.com/GaAs.html (last accessed December 6, 2007).

[10] Theodore R. Hoelter and Jeffrey B. Barton. “Extended short wavelength spectral response from InGaAs focal plane arrays.” Proceedings of SPIE -- Volume 5074. Infrared Technology and Applications XXIX, September 2003, 481-490.

[11] Indigo Systems Corporation. “Alpha^{TM} NIR User Manual.”

[12] Electro Optical Industries Inc. “Typical Detector Responsivity.” http://www.electro-optical.com/bb_rad/detector.htm (last accessed December 6, 2007).

[13] Inition Corporation. “Liteye LE-500.” http://www.inition.co.uk/inition/images/product_hmd_liteye_500_3.jpg (last accessed December 6, 2007).

[14] Sensor Unlimited. Sensors Unlimited Near-IR MicroCameras on UAVs. http://www.sensorsinc.com/downloads/PR_031705.pdf (last accessed December 6, 2007).

[15] Joseph P. Estrera, Timothy E. Ostromek, Antonio V. Bacarella, Wayne Isbell, Mike J. Iosue, Michael R. Saldana and Timothy R. Beystrum. “Advance image intensifier night vision system technologies: status and summary 2002.” Abstract obtained from Proceedings of the SPIE, Volume 4796 (2003).

[16] Vatsia, Mirshri, L. “Atmospheric Optical Environment,” Research and Development Technical Report ECOM-7023, September (1972).

[17] DARPA Public Release. http://www.darpa.mil/mto/solicitations/baa06-46/pdf/publicRelease.pdf (last accessed December 6 2007)

[18] Austin Richards. “Military and Homeland Security Applications for Shortwave Infrared Imaging.” Presentation to Naval Postgraduate School Physics Colloquium on 19 January 2007.

[19] Sensor Unlimited. “A Little Night Vision." http://www.sensorsinc.com/downloads/article_Adv.Imging_305.pdf (last accessed December 6, 2007).

[20] PTI Monochromator Model 101 User Manual.

[21] United States Patent Number 6,805,957. “Camouflage U.S. Marine Corps Utility Uniform: pattern, fabric and design.”

[22] D. Saravanan. “Camouflage for Warfare.” Applied Technology Journal, May 2007, 28-32.

[23] NASA Jet Propulsion Laboratory. http://speclib.jpl.nasa.gov/ (last accessed December 6, 2007).

[24] Gregory L. Matloff. “Deep Space Probe Deep Space Probes: To the Outer Solar System and Beyond.” Berlin: Springer, 2005.

[25] Patrick L. Barry and Tony Phillips. Artist's impression of a solar sail. http://www.nhsta.net/Information/NASA/solar_sail_art.jpg (last accessed December 6, 2007).

[26] Yoel Fink, Mehmet Bayindir, Fabien Sorin, Ayman F. Abouraddy, Jeff Viens, Shandon D. Hart and John D. Joannopoulos. "Metal-insulator-semiconductor optoelectronic fibres." Nature. October 14, 2004. p. 826.

[27] Richard V. Gregory, Timothy Hanks and Robert J. Samuels. "Dynamic Color Change Chameleon Fiber Systems The Next Step." National Textile Center Research Briefs – Materials Competency: June 2004.

[28] Timothy Hanks. Chameleon Fiber Project Website. http://facweb.furman.edu/~thanks/ntc/outline.html (last accessed December 6, 2007).

[29] Stephen S. Hardaker and Richard V. Gregory. "Progress toward dynamic color-responsive "chameleon" fiber systems." Materials Research Society Bulletin. August 2003.

[30] Trevor Nevitt Dupuy. "The Evolution of Weapons and Warfare." Cambridge, MA: Da Capo Press, 1990.

THIS PAGE INTENTIONALLY LEFT BLANK

INITIAL DISTRIBUTION LIST

1. Defense Technical Information Center
   Ft. Belvoir, Virginia

2. Dudley Knox Library
   Naval Postgraduate School
   Monterey, California

3. Ho Chee Leong
   Singapore Armed Forces (Army)
   Singapore

4. Professor Nancy Haegel
   Naval Postgraduate School
   Monterey, California

5. Professor Gamani Karunasiri
   Naval Postgraduate School
   Monterey, California

6. Mr Austin Richards
   FLIR Systems
   Santa Barbara, California